

On the External Validity of Average-Case Analyses of Graph Algorithms

Thomas Bläsius  

Karlsruhe Institute of Technology (KIT), Germany

Philipp Fischbeck  

Hasso Plattner Institute (HPI), University of Potsdam, Germany

Abstract

The number one criticism of average-case analysis is that we do not actually know the probability distribution of real-world inputs. Thus, analyzing an algorithm on some random model has no implications for practical performance. At its core, this criticism doubts the existence of *external validity*, i.e., it assumes that algorithmic behavior on the somewhat simple and clean models does not translate beyond the models to practical performance real-world input.

With this paper, we provide a first step towards studying the question of external validity systematically. To this end, we evaluate the performance of six graph algorithms on a collection of 2740 sparse real-world networks depending on two properties; the heterogeneity (variance in the degree distribution) and locality (tendency of edges to connect vertices that are already close). We compare this with the performance on generated networks with varying locality and heterogeneity. We find that the performance in the idealized setting of network models translates surprisingly well to real-world networks. Moreover, heterogeneity and locality appear to be the core properties impacting the performance of many graph algorithms.

2012 ACM Subject Classification Theory of computation → Graph algorithms analysis; Theory of computation → Randomness, geometry and discrete structures

Keywords and phrases Average Case, Network Models, Empirical Evaluation

Digital Object Identifier 10.4230/LIPICs...22

Related Version An extended abstract of this work was published at ESA 2022 [5].



© Thomas Bläsius and Philipp Fischbeck;

licensed under Creative Commons License CC-BY 4.0

Leibniz International Proceedings in Informatics

LIPICs Schloss Dagstuhl – Leibniz-Zentrum für Informatik, Dagstuhl Publishing, Germany

1 Introduction

The seminal papers of Cook in 1971 [20] and Karp in 1972 [35] establish that many fundamental combinatorial problems are NP-hard, and thus cannot be solved in polynomial time unless $P = NP$. Since then, the list of NP-hard problems is growing every year; see the book by Garey and Johnson [30] for an extensive list of problems that were shown to be hard in the early years of complexity theory.

Though the non-existence of polynomial time algorithms (unless $P = NP$) is major bad news, the concept of NP-hardness is limited to the worst case. It thus leaves the possibility of imperfect algorithms that fail sometimes but run correctly and in polynomial time on most inputs. Many algorithms used today are slow in the worst case but perform well on relevant instances. An early attempt to theoretically capture this “good in practice” concept is the *average-case analysis*. There, one assumes the input to be randomly generated and then proves a low failure probability or a good expected performance.¹ On that topic, Karp wrote in 1983 [36] that

One way to validate or compare imperfect algorithms for NP-hard combinatorial problems is simply to run them on typical instances and see how often they fail. [...] While probabilistic assumptions are always open to question, the approach seems to have considerable explanatory power [...]. (Karp in 1983)

With this promising starting point, one could have guessed that average-case analysis is an important pillar of algorithmic research. However, it currently plays only a minor role in theoretical computer science. The core reason for this was summarized by Karp almost forty years later in 2020 in the Lex Fridman Podcast.²

The field tended to be rather lukewarm about accepting these results as meaningful because we were making such a simplistic assumption about the kinds of graphs that we would be dealing with. [...] After a while I concluded that it didn’t have a lot of bite in terms of the practical application. (Karp in 2020)

At its core, this describes the issue that an average-case analysis is lacking *external validity*, i.e., the insights on randomly generated graphs do not transfer to practical instances.

The simplistic probabilistic assumption mentioned in the above quotes is that input graphs are drawn from the Erdős–Rényi model [28], where all edges exist independently at random with the same probability. This assumption has the advantages that it is as unbiased as possible and sufficiently accessible to allow for mathematical analyses. However, in its simplicity, it is unable to capture the rich structural properties present in real-world networks, leading to the lack of external validity.

That being said, since the beginnings of average-case considerations, there have been several decades of research in the field of network science dedicated to understanding and explaining properties observed in real-world networks. This in particular includes the analysis of random network models and the transfer of insights from these models to real networks; indicating external validity. Thus, we believe that it is time to revisit the question of whether

¹ We note that within the scope of this paper the term *average case* refers to exactly those situations where the input is drawn from some probability distribution. This includes proving bounds that hold with high probability (instead of in expectation), which would technically be better described as *typical case*. Moreover, it excludes the case of randomized algorithms on deterministic inputs.

² Transcript of the Lex Fridman Podcast #111. The quote itself starts at 1:39:59. For the full context, start at 1:37:28 (<https://youtu.be/K1lCr1fLuzs?t=5848>).

average-case analyses of graph algorithms can have external validity. With this paper, we present a first attempt at systematically studying this question.

Before describing our approach and stating our contribution, we want to give two examples from network science, where the existence of external validity is generally accepted.

Examples from Network Science. The Barabási–Albert model [3] uses the mechanism of *preferential attachment* to iteratively build a network. Each newly added vertex chooses a fixed number of neighbors among the existing vertices with probabilities proportional to the current vertex degrees. This simple mechanism yields *heterogeneous* networks, i.e., networks with power-law degree distributions where most vertices have a small degree while few vertices have very high degree.³ It is well known that networks generated by this model are highly artificial, exhibiting properties that are far from what is observed in real-world networks. Nonetheless, beyond the specific model, it is generally accepted that the mechanism of preferential attachment facilitates power-law distributions. Thus, assuming external validity, the Barabási–Albert model can serve as an explanation of why we regularly observe power-law distributions in real-world data. Moreover, whenever we deal with a process involving preferential attachment, we should not be surprised when seeing a power-law distribution.

The Watts–Strogatz model [45] first starts with a ring lattice, i.e., the vertices are distributed uniformly on a circle and vertex pairs are connected if they are sufficiently close. This yields a regular graph with high *locality*, i.e., all connections are short and we observe many triangles. Moreover, ring lattices have high diameter. The second step of the Watts–Strogatz model introduces noise by randomly rewiring edges. This diminishes locality by replacing local connections with potentially long-range edges. Watts and Strogatz demonstrate that only little locality has to be sacrificed before getting a small-world network with low diameter. Again, this model is highly artificial and thus far from being a good representation for real-world networks. However, it seems generally accepted that these observations have implications beyond the specific model, namely that there is a simple mechanism that facilitates the small-world property even in networks with mostly local connections. Thus, in real-world settings where random long-range connections are possible, one should not be surprised to observe the small-world property.

Contribution. We consider algorithms for six different problems that are known to perform better in practice than the worst-case complexity would suggest. We evaluate them on network models that allow for varying amounts of locality and heterogeneity.⁴ This shows us the impact of these two properties on the algorithms’ performance in the controlled and clean setting of generated networks. We compare this with practical performance by additionally evaluating the algorithms on a collection of 2740 sparse real-world networks. Our overall findings can be summarized as follows. Though the real-world networks yield a less clean and more noisy picture than the generated networks, the overall dependence of the performance on locality and heterogeneity coincides with surprising accuracy for most algorithms. This indicates that there is external validity in the sense that if, e.g., increasing locality in the network models improves performance, we should also expect better performance for real-world networks with high locality. Moreover, it indicates that locality

³ Barabási and Albert were not the first to study a preferential attachment mechanism; see, e.g., Price’s model [24]. However, there is no doubt that their highly influential paper [3] popularized the concept.

⁴ For non-local networks, we use the Erdős–Rényi and the Chung–Lu model for homogeneous and heterogeneous degree distributions, respectively. For local networks, we use geometric inhomogeneous random graphs (GIRGs), which let us vary the amount of locality and heterogeneity.

and heterogeneity are the core properties to impact the performance for many networks. More specifically, we have the following findings for the different algorithms.

- The bidirectional BFS for computing shortest paths in undirected networks runs in sublinear time except on homogeneous and local networks. The running times are very similar for the generated and real-world networks.
- The iFUB algorithm [22] for computing the diameter performs well on heterogeneous networks when starting it with a vertex of highest degree. When choosing the starting vertex via 4-sweep instead, it additionally performs well on networks that are homogeneous and local. This trend is true for generated and real-world networks.
- The dominance rule, a reduction rule for the vertex cover problem, performs well for networks that are sufficiently local or heterogeneous. Again, this trend can be observed for generated and real-world networks.
- The Louvain algorithm [4] for clustering graphs requires few iterations for most generated and real-world networks independent of locality and heterogeneity. Though the experiments indicate that low locality increases the chance for hard instances, the results are inconclusive as locality and heterogeneity do not seem to be the main deciding factors.
- The run time for enumerating all maximal cliques mainly depends on the output size, which can be exponential in the worst-case. Surprisingly, all generated networks have at most m maximal cliques, where m is the number of edges. Moreover, the number decreases for increasing locality. We make the identical observation (not only asymptotically but with the same constant factors) on 93 % of the real-world networks.
- A reduction rule for computing the chromatic number of a graph with clique number ω is to reduce it to its ω -core [43]. It works well if the degeneracy is low compared to ω . For generated and real-world networks, the clique number and the degeneracy behave almost identical, both increasing for higher locality and heterogeneity. The reduction rule itself has decent performance on very heterogeneous networks. On less heterogeneous networks, it performs better for higher localities. In addition, we observe an interesting threshold behavior in the average degree, depending on the locality, for the generated networks.

Our insights for the specific algorithms are interesting in their own right, independent of the question of external validity. Moreover, our experiments led to several interesting findings that are beyond the core scope of this paper. These can be found in the appendix.

In Section 2, we introduce some basic notation and formally define measures for heterogeneity and locality. In Section 3, we describe the set of real-world and generated networks we use in our experiments. Section 4 compares generated and real-world networks for the different algorithms. Related work as well as our insights specific to the algorithms are discussed in this section. In Section 5 we conclude with a discussion of our overall results.

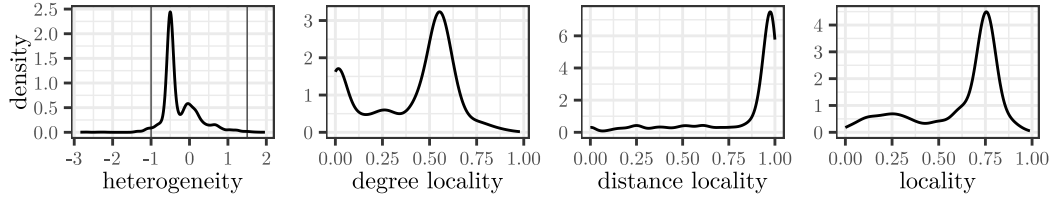
Our source code is available on GitHub⁵. It is additionally archived at Zenodo⁶, together with a docker image for easier reproducibility. The latter repository additionally includes the real-world network data set as well as all generated data (networks and statistics).

2 Basic Definitions, Heterogeneity, and Locality

Let $G = (V, E)$ be a graph. Throughout the paper, we denote the number of vertices and edges with $n = |V|$ and $m = |E|$. For $v \in V$, let $N(v) = \{u \mid \{u, v\} \in E\}$ be the *neighborhood*

⁵ <https://github.com/thobl/external-validity>

⁶ <https://doi.org/10.5281/zenodo.8058432>



■ **Figure 1** The density (kernel density estimation) of heterogeneity, degree locality, distance locality, and locality of the networks in our data set of real-world networks.

of v , and let $\deg(v) = |N(v)|$ be the *degree* of v . Additionally, $N[v] = N(v) \cup \{v\}$ is the *closed neighborhood* of v . An edge $e \in E$ is a *bridge* if $G - e$ is disconnected, where $G - e$ denotes the subgraph induced by $E \setminus \{e\}$.

2.1 Heterogeneity

We define the *heterogeneity* of a graph as the logarithm (base 10) of the coefficient of variation of its degree distribution. To make this specific, let $\mu = \frac{1}{n} \sum_{v \in V} \deg(v)$ be the average degree of $G = (V, E)$, and let $\sigma^2 = \frac{1}{n} \sum_{v \in V} (\deg(v) - \mu)^2$ be the variance. Then, the *coefficient of variation* is σ/μ , i.e., the standard deviation relative to the mean. Thus, the heterogeneity is $\log_{10}(\sigma/\mu)$. The resulting distribution of heterogeneity values is shown in Figure 1. The figure includes thresholds for extreme heterogeneity values that we use to filter real-world graphs in our visualizations; see Section 4 for details.

2.2 Locality

We define locality as a combination of two different notions of locality on edges. The degree locality of an edge is high if its endpoints have many common neighbors. This is similar to the commonly known local clustering coefficient of vertices. Our second measure, the distance locality, captures the locality of edges that do not have common neighbors. In the following, we first introduce these parameters. The subsequent discussion helps to interpret them and justifies our choices. For the distribution of the different locality values over the networks see Figure 1.

Degree Locality. For $u, v \in V$, let $\deg(u, v) = |N(u) \cap N(v)|$ be the *common degree* of u and v . For a non-bridge edge $\{u, v\} \in E$ the *degree locality* is defined as

$$L_{\deg}(\{u, v\}) = \frac{\deg(u, v)}{\min(\deg(u), \deg(v)) - 1}.$$

The -1 in the denominator accounts for the fact that u is always in v 's neighborhood but never in the common neighborhood. With this, we get $L_{\deg}(\{u, v\}) \in [0, 1]$ and $L_{\deg}(\{u, v\}) = 0$ if and only if the neighborhoods of u and v are disjoint. Moreover, $L_{\deg}(\{u, v\}) = 1$ if and only if u is only connected to v and to neighbors of v or vice versa. Essentially, $L_{\deg}(\{u, v\})$ measures in how many triangles $\{u, v\}$ appears. Note that the denominator is never 0 as we require the edge to not be a bridge and thus u and v both have degree at least 2.

The *degree locality* $L_{\deg}(G)$ of G is the average degree locality over all non-bridge edges.

Distance Locality. For $u, v \in V$, let $\text{dist}(u, v)$ be the distance between u and v in G . If $\text{dist}(u, v) = 1$, i.e., $\{u, v\}$ is an edge, we are additionally interested in the detour we have

to make when not allowing to use the direct edge $\{u, v\}$. To this end, we define the *detour distance* $\text{dist}^+(u, v)$ to be the distance between u and v in $G - \{u, v\}$.

For a set of vertex pairs $P \subseteq \binom{V}{2}$ we define $\text{dist}(P)$ to be the *average distance* of P , i.e.,

$$\text{dist}(P) = \frac{1}{|P|} \sum_{\{u, v\} \in P} \text{dist}(u, v).$$

Analogously, we define $\text{dist}^+(P)$ to be the average detour distance of P .

Let $\overline{E} = \binom{V}{2} \setminus E$ be the *non-edges* of G and assume that $\overline{E} \neq \emptyset$. Note that $\text{dist}(\overline{E}) \geq 2$, as non-adjacent vertex pairs have distance at least 2. Assume for now that $\text{dist}(\overline{E}) > 2$. For a non-bridge edge $\{u, v\} \in E$, we define the *distance locality* as

$$L_{\text{dist}}(\{u, v\}) = 1 - \frac{\text{dist}^+(u, v) - 2}{\text{dist}(\overline{E}) - 2}.$$

Note that the numerator is 0 if and only if u and v have a common neighbor, which yields $L_{\text{dist}}(\{u, v\}) = 1$. Moreover, we have $L_{\text{dist}}(\{u, v\}) = 0$ if and only if the detour distance between u and v equals the average distance between non-adjacent vertex pairs in G . Finally, $L_{\text{dist}}(\{u, v\})$ can be negative if $\{u, v\}$ connects a vertex pair that is otherwise more distant than one would expect for a non-adjacent vertex pair. Thus, the distance locality essentially measures how short the edge $\{u, v\}$ is compared to the average distance in the graph. In the special case of $\text{dist}(\overline{E}) = 2$, we define $L_{\text{dist}}(\{u, v\}) = 0$.

The *distance locality* $L_{\text{dist}}(G)$ of G is the maximum of 0 and the average distance locality over all non-bridge edges.

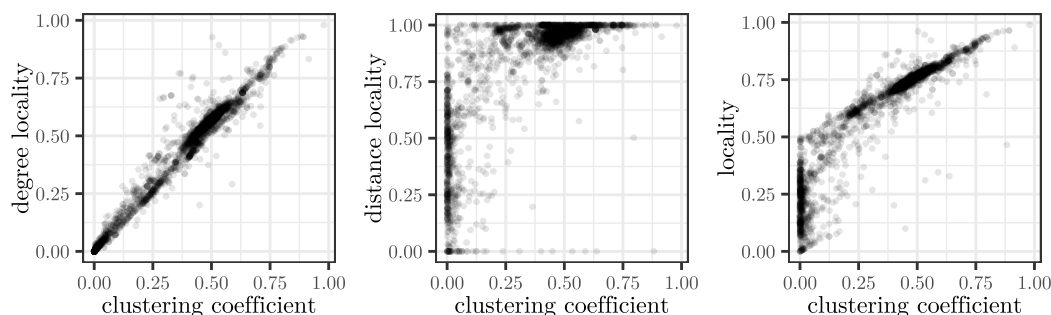
Locality. The *locality* $L(G)$ of G is the average of the degree and the distance locality, i.e., $L(G) = (L_{\text{deg}}(G) + L_{\text{dist}}(G))/2$.

To interpret this parameter, let $L(e) = \frac{1}{2}(L_{\text{deg}}(e) + L_{\text{dist}}(e))$ be the *edge locality* of a non-bridge edge $e = \{u, v\} \in E$. Note that $L(G)$ is basically⁷ the average of all edge localities. Observe that $L_{\text{deg}}(e) > 0$ and $L_{\text{dist}}(e) = 1$ if u and v have a common neighbor. Otherwise $L_{\text{deg}}(e) = 0$ and $L_{\text{dist}}(e) < 1$. Thus, we in particular get the following regimes for $L(e)$.

- $L(e) \in (\frac{1}{2}, 1]$ if u and v have a common neighbor. The more common neighbors u and v have, the higher $L(e)$.
- $L(e) \in (0, \frac{1}{2})$ if u and v have no common neighbor but are closer in $G - e$ than the average non-adjacent vertex pair in G . The closer u and v are, the higher $L(e)$.

Discussion & Comparison to the Clustering Coefficient. The degree locality is closely related to the commonly known local clustering coefficient. Note that the degree locality (like the clustering coefficient) only cares for triangles. Though this is desirable in some cases, it does not provide a good separation between graphs with few triangles. An extreme case are bipartite graphs that have no triangles and thus degree locality and clustering coefficient 0. However, we would regard, e.g., grids as highly local. The distance locality solves this issue by essentially defining a measure of locality that distinguishes between graphs of low degree locality. Figure 2 shows a comparison of our locality values to the local clustering coefficient. Note how, for high values, the locality behaves as the clustering coefficient (scaled by a factor of 2), while it provides additional separation for networks with clustering close to 0. See section B.1 for an extended discussion.

⁷ This is true unless the average over all distance localities is negative, in which case we capped the distance locality at 0. See Section B.2 for a detailed discussion.



■ **Figure 2** Comparison of the average local clustering coefficient to the degree locality (left), the distance locality (center), and the locality (right). Each dot represents one network from our data set of real-world networks.

Limitations. We note that our locality definition has some limitations, e.g., it is undefined for trees as trees have no non-bridge edges. However, these limitations do not pose an issue in the context of this paper; see Section B.2 for more details.

Computing the Locality. Computing the distance locality efficiently is not straight-forward. In Section B.3, we show how to compute it by computing two values for a given graph: the average distance between all vertex pairs, and the average detour distance over all non-bridge edges. The latter can be computed exactly in reasonable time using some insights from Section 4.1 (see Section B.3 for details).

For the average distance between all vertex pairs, we use an approximation. Specifically we implemented the algorithm by Chechik, Cohen, and Kaplan [13]. We observed that there is a simple way to significantly improve its approximation ratio by conditioning on random choices that have been made earlier in the algorithm. Additionally, we compared the algorithm with the straight-forward method of computing the shortest path between uniformly sampled vertex pairs. Our experiments indicate that the preferable method depends on the locality and heterogeneity of a network. Though these results are interesting in their own right, they are somewhat beyond the scope of this paper and thus deferred to Section C.

3 Networks

3.1 Real-World Networks

We use 2740 graphs from Network Repository [40], which we selected as follows. We started with all networks with at most 1 M edges and reduced each network to its largest connected component. We removed multi-edges and self-loops and ignored weights or edge directions. We tested the resulting connected, simple, undirected, and unweighted graphs for isomorphism and kept only one copy for each group of isomorphic networks. This resulted in 2977 networks. From this we removed 237 networks for different reasons.

- We removed 111 networks that were randomly generated and thus do not count as real-world networks.⁸

⁸ Finding generated networks was done manually by searching for suspicious naming patterns or graph properties. For each candidate, we checked its source to verify that it is a generated network. Though we checked thoroughly, there are probably a few random networks hiding among the real-world networks.

- We removed 2 trees. They are not very interesting, and locality is not defined for trees.
- We removed 124 graphs with density at least 10%. Our focus lies on sparse graphs and network models for sparse graphs. Thus, dense graphs are out of scope.

3.2 Random Networks

We use three random graph models to generate networks; the Erdős–Rényi model [28] (non-local and homogeneous), the Chung–Lu model [16, 17] (non-local and varying heterogeneity), and the GIRG model [12] (varying locality and heterogeneity). For the latter, we use the efficient implementation in [9]. In the following we briefly define the models, discuss the model choice, and specify what networks we generate.

Network Model Definitions. Given n and m , the *Erdős–Rényi model* draws a graph uniformly at random among all graphs with n vertices and m edges.

Given n weights w_1, \dots, w_n with $W = \sum w_v$, the *Chung–Lu model* generates a graph with n vertices by creating an edge between the u th and v th vertex with probability

$$p_{u,v} = \min \left\{ \frac{w_u w_v}{W}, 1 \right\}.$$

The expected degree of v is then roughly proportional to w_v . We use weights that follow a power law. Specifically, for a constant c and a power-law exponent $\beta > 2$, we choose

$$w_v = c \cdot v^{-\frac{1}{\beta-1}}.$$

Thus, the parameters are the number of vertices n , the expected average degree (controlled via c), and the power-law exponent β . The latter controls the heterogeneity of the network: heterogeneity is high for small β and for $\beta \rightarrow \infty$ we get uniform weights.

The *GIRG model* (geometric inhomogeneous random graphs) augments the Chung–Lu model with an underlying geometry. In a first step, each vertex v is mapped to a random position \mathbf{v} in some d -dimensional ground space. Let $\|\mathbf{u} - \mathbf{v}\|$ denote the distance between vertices u and v in that space. Then, for a so-called *temperature* $T \in (0, 1)$, the vertices u and v are connected with probability

$$p_{u,v} = \min \left\{ \left(\frac{1}{\|\mathbf{u} - \mathbf{v}\|^d} \cdot \frac{w_u w_v}{W} \right)^{\frac{1}{T}}, 1 \right\}.$$

Additionally, for $T = 0$, a threshold variant is obtained, with $p_{u,v} = 1$ if $\|\mathbf{u} - \mathbf{v}\|^d \leq w_u w_v / W$ and $p_{u,v} = 0$ otherwise. For the weights, we use the same power-law weights as for the Chung–Lu model. As ground space, we usually use a 2-dimensional torus $\mathbb{T}^2 = [0, 1] \times [0, 1]$ with maximum norm, which is basically just a unit square with distances wrapping around in both dimensions. More precisely, for $\mathbf{u} = (x_u, y_u) \in \mathbb{T}$ and $\mathbf{v} = (x_v, y_v) \in \mathbb{T}$, we have $\|\mathbf{u} - \mathbf{v}\| = \max\{\min\{|x_u - x_v|, 1 - |x_u - x_v|\}, \min\{|y_u - y_v|, 1 - |y_u - y_v|\}\}$. With this, the parameters that remain to be chosen for the GIRG model are the same as for the Chung–Lu model plus the temperature T , which mainly controls the locality.

Discussion of the Network Models. We note that there is a plethora of network models out there. So, why did we choose these particular models? To answer this, consider two different use-cases for network models. First, to explain why and how certain properties emerge in networks assuming some mechanism existing in the real world. Secondly, to draw conclusions from the existence of certain properties in a network.

An example of the first perspective is the Barabási–Albert model [3], where the simple and believable mechanism of preferential attachment yields a power-law degree distribution.

The second perspective is what we are concerned with in this paper. We do not aim at explaining how locality or heterogeneity emerge in networks. Instead we want to study the implications of these properties on algorithmic performance. For this purpose, we believe that it is crucial for the model to be maximally unbiased beyond the explicitly assumed properties. Ideally, one uses the maximum entropy model with respect to the given constraints.

With this in mind, note that the Erdős–Rényi model draws graphs uniformly at random, given the number of vertices and edges. This is the maximum entropy model and thus maximally unbiased with the constraints that the number of vertices and edges are given.

For graphs whose degree distribution follows a power law, one could use the above mentioned Barabási–Albert model. However, this model is biased in all sorts of ways that go beyond assuming a power-law degree distribution (e.g., the resulting graphs are k -degenerate for average degree $2k$). The maximum entropy model for graphs with power-law distribution is the (soft) configuration model [42]. The Chung–Lu model we use is close to the soft configuration model but much easier to work with. Thus, it is a good compromise between being unbiased beyond the assumptions we want to make and being able to efficiently generate networks or conduct theoretical analyses.

Finally, the GIRG model enhances the Chung–Lu model with locality by assuming an underlying geometry. Though the model is set up to be as unbiased as possible beyond this assumption, we are not aware of a formal proof for this. Moreover, it is up for debate whether a geometry is the best way to introduce locality. Instead, one could, e.g., assume a fixed set of communities like in the stochastic block model [33]. However, assigning vertices to geometric positions seems like the most straight-forward way of introducing a smooth notion of similarity. Thus, at the current state of research, we believe that assuming an underlying geometry is the best way to achieve locality for our purpose. As an added bonus, the amount of locality can be controlled with just a single parameter (the temperature) and there is an efficient generator [9] readily available.

Generated Networks & Parameter Choices. For all models, we generate networks with $n = 50\text{ k}$ vertices and (expected) average degree 10. For the power-law exponent β in Chung–Lu graphs and GIRGs as well as for the temperature T in GIRGs we chose the values shown in Figure 3, yielding a rather uniform distribution of heterogeneity and locality.

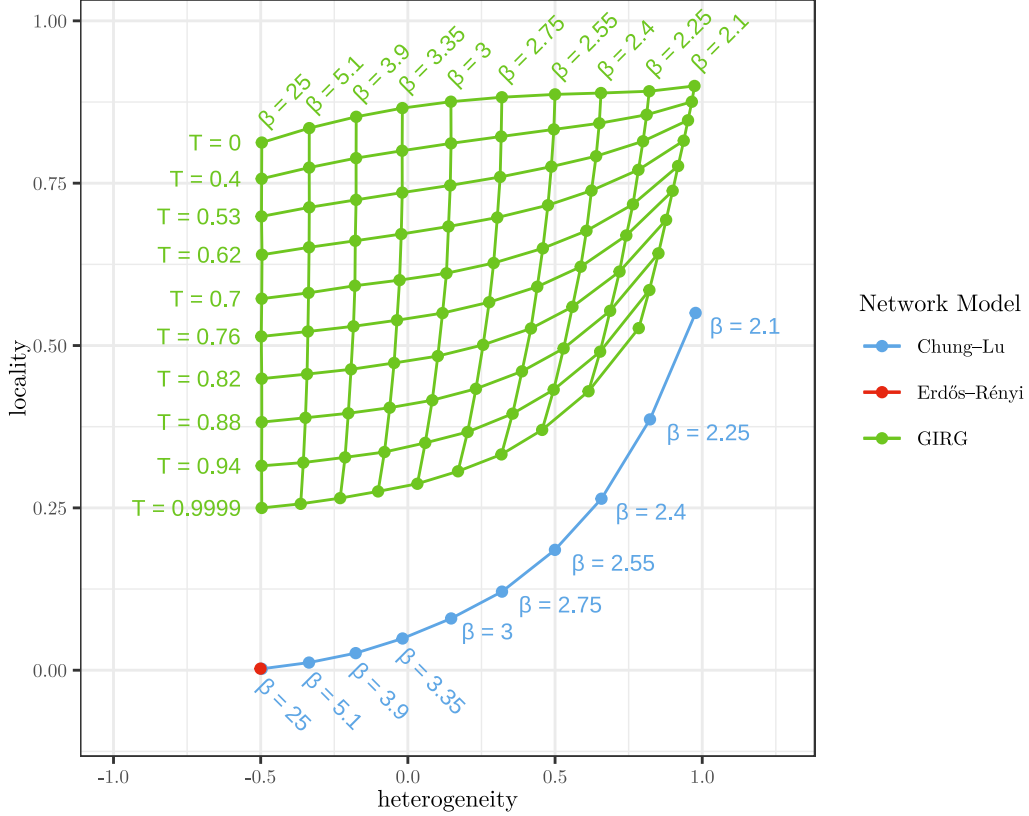
Note that we have ten different values for each of the parameters β and T , which results in 100 different parameter configurations for GIRGs, ten configurations for Chung–Lu graphs, and a single configuration for Erdős–Rényi graphs. For each of these 111 configurations, we generated five networks. In the plots, we always use a single dot for each configuration representing the average over five individual networks.

As for the real-world networks, we reduce each generated graph to its largest connected component. With the above parameter choices, this does not change the size of the networks by too much; see Section D.1.

In Section 4.6, we additionally consider networks of average degree 20, using otherwise the same parameter settings.

We note the power-law weights converge to uniform weights for $\beta \rightarrow \infty$. Thus, in the limit, the probability distribution of the Chung–Lu model (almost)⁹ coincides with that

⁹ The distributions are not exactly the same, as the Chung–Lu model achieves the desired number of edges only in expectation. But conditioning on the average degree having its expected value, the two



■ **Figure 3** Heterogeneity and locality of the generated networks from the different models. Each point is the average of five samples with the given parameter configuration.

of the Erdős-Rényi model. It is thus not surprising that the Erdős-Rényi graphs and the Chung-Lu graphs with $\beta = 25$ occupy almost the same spot in Figure 3.

Geometric Ground Space. We usually use a torus with dimension $d = 2$ as ground space of the GIRG model. For temperature $T = 0$, we have a threshold model where two vertices are connected if and only if their distance is sufficiently small compared to the product of their weights. Thus, for $\beta \rightarrow \infty$ this converges to the commonly known model of random geometric graphs; just on the torus \mathbb{T} instead the more commonly used unit square in the Euclidean plane. Moreover, for smaller β , we basically get hyperbolic random graphs [37]; just in one more dimension than usual.

The reason for using a torus instead of a square in the GIRG model is that a square leads to special situations close to the boundary while the torus wraps around and thus is completely symmetric. This usually simplifies theoretic analysis without changing too much otherwise. Interestingly, we observe in our experiments that the choice of torus vs. square makes a substantial difference for computing the diameter; see Section 4.2. To make this comparison, we additionally generated five GIRGs with a square as ground space for each of the parameter settings; see Section D.2 for details on how we generated these networks.

coincide.

4 Comparison Between the Models and Real-World Networks

Each of the following subsections compares the performance of a different algorithm between generated and real-world networks. For the cost c of the algorithm, we plot c depending on heterogeneity and locality using color to indicate the cost; see, e.g., Figure 4. The left and middle plot show one data point for each parameter setting of the models and each real-world network, respectively. The right plot aggregates real-world networks with similar locality and heterogeneity. Each point represents a number of networks indicated by its radius (log scale). We regularly assume the cost c to be polynomial in m (or n), i.e., $c = m^x$, and plot $x = \log_m c$. In this case, the color in the left and right plot shows the mean exponent x aggregated over the networks.

The set of real-world networks contains some networks with extreme heterogeneity; their inclusion in the plots would squeeze the non-extreme data points together and make interpretation of the middle and right plot more difficult. Thus, in these plots we only consider real-world networks with a heterogeneity value between -1.0 and 1.5 . We refer to Appendix F for full versions of such plots including all networks with extreme heterogeneity. This restriction only affects such plots; in our statistics and discussions, we consider all real-world networks, including those with extreme heterogeneity.

4.1 Bidirectional Search

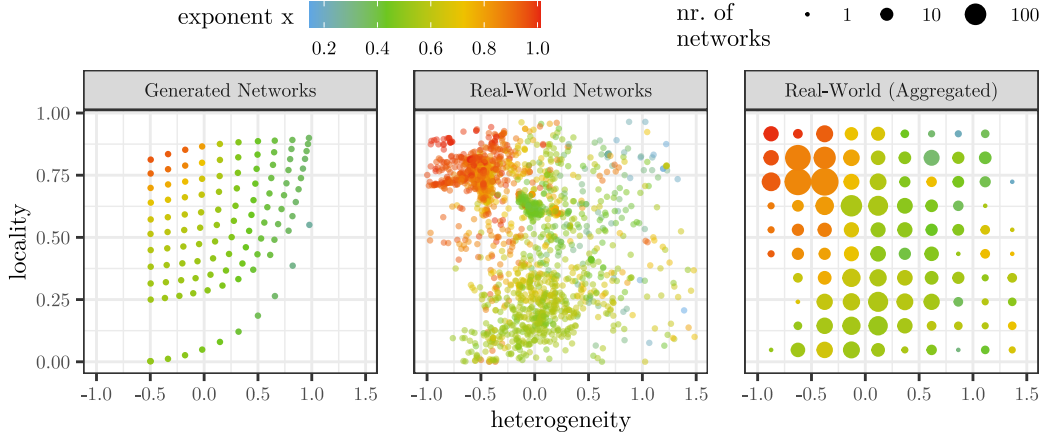
We can compute a shortest path between two vertices s and t using a *breadth first search* (*BFS*). The BFS explores the graph layer-wise, where the i th layer contains the vertices of distance i from s . By *exploring* the i th layer, we refer to the process of iterating over all edges with an endpoint in the i th layer, thereby finding layer $i + 1$. The search can stop once the current layer contains t .

The *bidirectional BFS* alternates the exploration of layers between a *forward BFS* from s and a *backward BFS* from t . The alternation strategy we study here greedily applies the cheaper of the two explorations in every step. The cost of exploring a layer is estimated via the sum of degrees of vertices in that layer. The search stops once the current layers of forward and backward search intersect. The resulting algorithm is called *balanced bidirectional BFS* [11], which we often abbreviate with just *bidirectional BFS* in the following.

The cost c for the bidirectional BFS is the average number of edge explorations over 100 random st -pairs. Note that $c \leq 2m$, as each edge can be explored at most twice; once from each side. Figure 4 shows the exponent x for $c = m^x$ depending on heterogeneity and locality.

Impact of Locality and Heterogeneity. For the generated data, we see that networks with high locality and homogeneous degree distribution (top left corner) have an exponent of around 1 (red). Thus, the cost of the bidirectional BFS is roughly m , which matches the worst-case bound. If the network is heterogeneous (right) or less local (bottom), we get significantly lower exponents of around 0.5, indicating a cost of roughly \sqrt{m} . The cost is particularly low for very heterogeneous networks. Overall, we get a strict separation between hard (high locality, low heterogeneity) and easy (low locality or high heterogeneity) instances.

For real-world networks, we observe the same overall behavior that instances that are local and homogeneous tend to be hard while all others tend to be easy. There are only few exceptions to this, indicating that the heterogeneity and locality are usually the crucial properties impacting the performance of the bidirectional BFS.



■ **Figure 4** The exponent x of the average cost $c = m^x$ of the bidirectional BFS over 100 st -pairs.

Discussion. Borassi and Natale [11] found that the bidirectional BFS is surprisingly efficient on many networks, which they used to efficiently compute the betweenness centrality. Additionally, they studied the bidirectional BFS theoretically on random network models where the edges are drawn independently, i.e., when there is no locality. They in particular prove that the search requires with high probability only $O(\sqrt{n})$ time for degree distributions with bounded variance. This includes the Erdős–Rényi model, and the Chung–Lu or the configuration model with power-law degree-distribution with power-law exponent $\beta \geq 3$. For $\beta \in (2, 3)$ (unbounded variance), the bound is $O(n^x)$ for $x \in (0.5, 1)$.¹⁰

For graphs with locality, it is known that the bidirectional BFS requires linear ($x = 1$) and sublinear ($x \in (0.5, 1)$)¹⁰ time on geometric random graphs in Euclidean and hyperbolic space, respectively [8]. We note that geometric random graphs in Euclidean and hyperbolic space essentially correspond to the top-left and top-right corner of Figure 4, as they can be viewed as special cases of GIRGs without or with heterogeneity, respectively.

Overall, the theoretical results on network models cover all four corners of the space spanned by heterogeneity and locality. Moreover, the predictions on the models match the observations on real-world networks, i.e., for most networks, the practical run time of the bidirectional BFS is not surprising but as expected. This indicates that locality and heterogeneity are the core deciding features for the performance of the bidirectional BFS.

4.2 Diameter

The *eccentricity* of $s \in V$ is $\max_{t \in V} \text{dist}(s, t)$, i.e., the distance to the vertex farthest from s . The *diameter* of the graph G is the maximum eccentricity of its vertices. It can be computed using the *iFUB algorithm* [22]. It starts with a root $r \in V$ from which it computes the BFS tree T . It then processes the vertices bottom up in T and computes their eccentricities using a BFS per vertex. This process can be pruned when the distance to r is sufficiently small compared to the largest eccentricity found so far. Pruning works well if r is a central vertex

¹⁰We note that the bounds for heterogeneous networks consider the worst-case over all st -pairs (which is dominated by the maximum degree for low power-law exponents) while our experiments consider the average over 100 random st -pairs. This explains why the theoretic bounds, though sublinear, seem to be worse than the empirical bounds.

in the sense that it has low distance to many vertices and a shortest path between distant vertices gets close to r .

There are different strategies of choosing the central vertex r . The *iFUB+hd* algorithm simply chooses a vertex of highest degree as starting vertex. A more sophisticated way of selecting r works as follows. A *double sweep* [39] starts with a vertex u , chooses a vertex v at maximum distance from u , and returns a vertex w from a middle layer of the BFS tree from v . A *4-sweep* [22] consists of two double sweeps, starting the second sweep with the result w of the first sweep. The *iFUB+4-sweep* algorithm chooses r by doing a 4-sweep from a vertex of maximum degree.

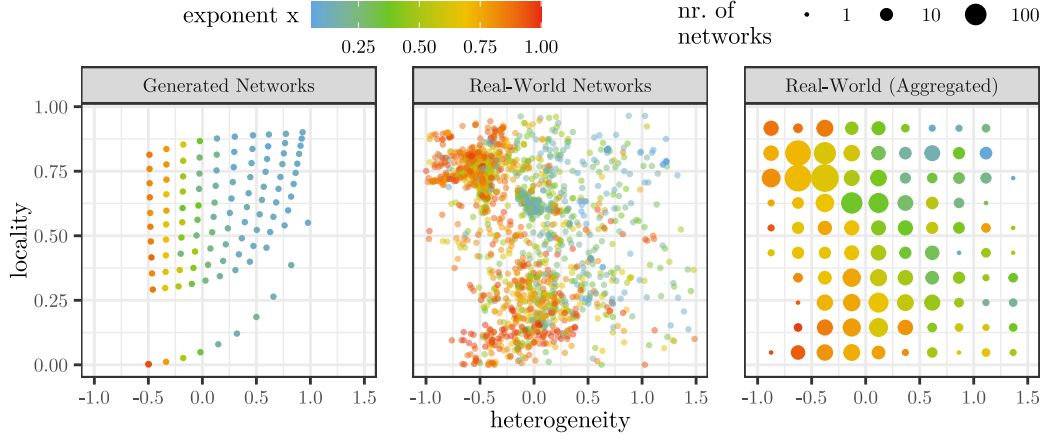
The *cost* c of iFUB+hd and iFUB+4-sweep is the number of BFSs it performs (including the four initial BFSs of the 4-sweep for iFUB+4-sweep). Note that $c \leq n$. Figure 5 shows the exponent x for $c = n^x$ depending on heterogeneity and locality. For iFUB+hd and iFUB+4-sweep, 17 and 16 real-world networks, respectively, are excluded from the plots as they exceeded the time limit of 30 min. The GIRG model uses a square as ground space instead of the usual torus; see discussion below for details.

Impact of Locality and Heterogeneity. The general dependence is the same for generated and real-world networks. For iFUB+hd (Figure 5a), an almost linear number of BFSs is required for networks lacking heterogeneity. On heterogeneous networks, i.e., if there are vertices of high degree, the number of BFSs is substantially sublinear. The more sophisticated iFUB+4-sweep variant (Figure 5b) additionally performs well on homogeneous networks with locality. Observe that the picture for real-world networks shows some noise, which indicates that there are properties besides locality and heterogeneity that impact the performance. We note, however, that this observation agrees with the models, where we get highly varying exponents for individual parameter settings, e.g., for iFUB+4-sweep on the five GIRGs with power-law exponent $\beta = 3.35$ and temperature $T = 0.62$, we get exponents ranging from 0.18 to 0.77 for the five generated instances.

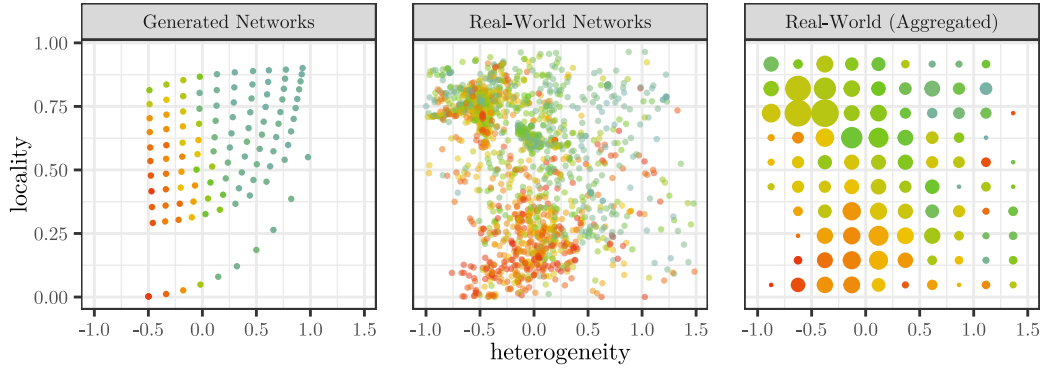
Impact of the Ground Space: Torus vs. Square. As mentioned in Section 3.2, the default ground space for the GIRG model is a torus. Though this might seem less natural than using a unit square, using the torus often simplifies theoretical analysis while not making a big difference otherwise. However, in the particular case of the iFUB+4-sweep algorithm, the ground space makes a significant difference. Figure 5c compares the efficiency of iFUB+4-sweep between torus-GIRGs and square-GIRGs.

Observe that the difference mainly shows for homogeneous and local networks (top-left corner), where iFUB+4-sweep requires an almost linear number of BFSs on torus-GIRGs, while being sublinear for square-GIRGs (as we have already observed in Figure 5b). This difference can be explained as follows. For square-GIRGs, the 4-sweep can find a vertex in the center of the ground space, which has relatively low distance to many vertices. As mentioned above, starting iFUB from such a vertex lets us prune the search early. In a torus, however, all points are identical and thus homogeneous torus-GIRGs do not have central vertices, rendering the iFUB approach ineffective.

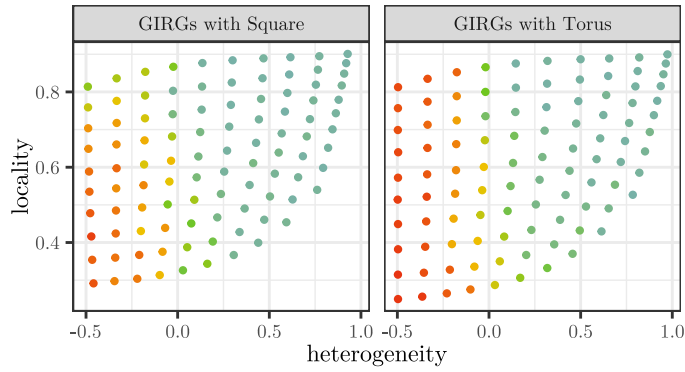
As mentioned above, iFUB+4-sweep performs well on most homogeneous and local real-world networks (Figure 5b). This indicates that square-GIRGs are a better representation for these networks than torus-GIRGs. There are, however, exceptions. Three such cases are the local and homogeneous networks `man_5976`, `tube1`, and `barth4` with exponents of 0.894, 0.873, and 0.89 respectively. Interestingly, all three graphs exhibit torus-like structures in the sense that they “wrap around” in some way, which obstructs the existence of a central vertex;



(a) Results for the iFUB+hd algorithm; 17 real-world networks are excluded due to timeout.

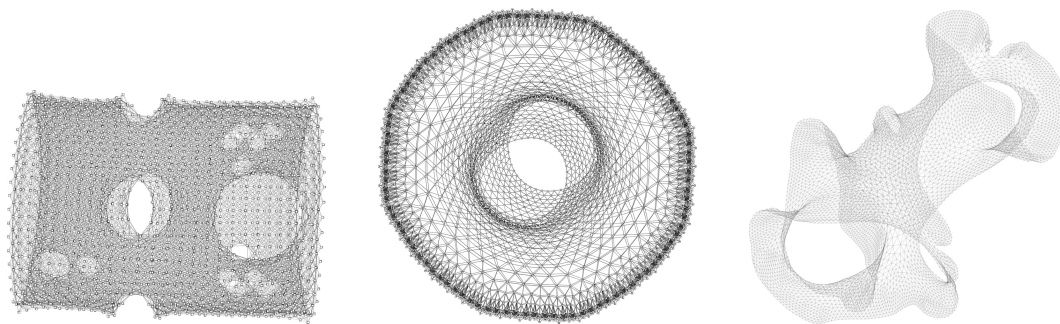


(b) Results for the iFUB+4-sweep algorithm; 16 real-world networks are excluded due to timeout.



(c) Comparison between torus and square as GIRG ground space for the iFUB+4-sweep algorithm.

Figure 5 The exponent x of the number of BFSs $c = n^x$ of the iFUB algorithms. Different from the rest of the paper, the GIRG ground space is a square instead of a torus.



■ **Figure 6** Graph drawings of the real-world networks `man_5976`, `tube1`, and `barth4` (from left to right). The graphs were drawn with the OGDF implementation [15] of the FM³ algorithm [31].

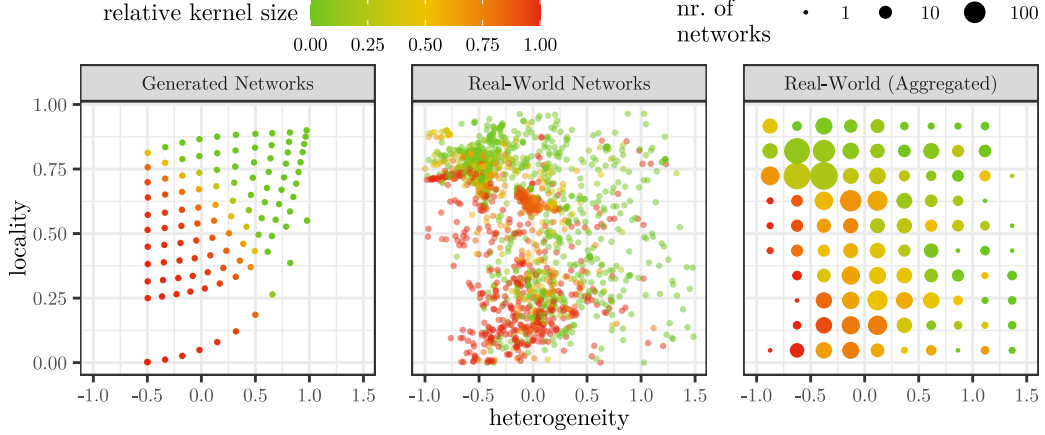
see Figure 6. Thus, also in this case, the predictions of the models match the real-world behavior.

4-Sweep Lower Bound. Diameter approximation methods such as the double sweep lower bound are known to perform well on real-world graphs [21, 39] and heterogeneous graph models [10]. As our experiments involve doing a 4-sweep anyways, we report the quality of the resulting 4-sweep lower bounds on our data set of real-world networks. We know the exact diameter for 2726 real-world networks (no timeout in iFUB+hd or iFUB+4-sweep). The 4-sweep lower bound matched the diameter for 2218 (81 %) of these networks. For 2703 (99 %) networks, the difference between the lower bound and the exact diameter is at most 2.

Discussion. The problem of computing the diameter of a graph is closely related to the all pairs shortest path (APSP) problem, i.e., computing the distance between all pairs of points. It is an open problem whether one can compute the diameter of arbitrary graphs faster than APSP [18]. The best known algorithms for APSP run in time $O(n^\omega)$ with $\omega < 2.38$ [2] or $O(nm)$. Both running times are infeasible for large real-world networks.

In practice, however, Crescenzi, Grossi, Habib, Lanzi, and Marino [22] introduced the iFUB algorithm and demonstrate that it performs much better on most real-world networks than the worst case suggests. They note that it works particularly well on networks with high difference between radius and diameter. This corresponds to the existence of a central vertex with eccentricity close to half the diameter. Our experiments confirm this and provide the following more detailed picture. First, in heterogeneous networks, the high degree nodes serve as central vertices. The results of Borassi, Crescenzi, and Trevisan [10] provide a theoretical foundation for this phenomenon. They in particular show that heterogeneous Chung–Lu graphs allow the computation of the diameter in sub-quadratic time, indeed using a vertex of high degree as central vertex. Second, for homogeneous networks, locality facilitates the existence of a central vertex, unless the graph exhibits a toroidal structure.

Our results point to some practical as well as theoretical open questions. The highest potential for practical improvements can be achieved by focusing on homogeneous graphs without locality or with a toroidal underlying geometry. Erdős–Rényi graphs or random geometric graphs with a torus as underlying geometry may help guide the development of such an algorithm. Moreover, it would be interesting to strengthen the theoretical foundation by complementing the above results by Borassi et al. [10] on Chung–Lu graphs to network models exhibiting locality (homogeneous as well as heterogeneous).



■ **Figure 7** The relative kernel size of the vertex cover domination rule.

4.3 Vertex Cover Domination

A vertex set $S \subseteq V$ is a *vertex cover* if every edge has an endpoint in S , i.e., removing S from G leaves a set of isolated vertices. We are interested in finding a vertex cover of minimum size. For two adjacent vertices $u, v \in V$, we say that u *dominates* v if $N[v] \subseteq N[u]$. The *dominance rule* states that there exists a minimum vertex cover that includes u . Thus, one can reduce the instance by including u in the vertex cover and removing it from the graph.

To evaluate the effectiveness of the dominance rule, we apply it exhaustively, i.e., until no dominant vertices are left. Moreover, we remove isolated vertices. We refer to the number c of vertices in the largest connected component of the remaining instances as the *kernel size*. Figure 7 shows the *relative kernel size* c/n with respect to locality and heterogeneity.

Impact of Locality and Heterogeneity. We see a sharp separation for the generated networks. For low locality and heterogeneity (bottom left), the reduction rule cannot be applied. For high locality and heterogeneity (top right), the dominance rule completely solves the instance. For real-world networks, the separation is less sharp, i.e., there is a larger range of locality/heterogeneity values in the middle where the dominance rule is effective sometimes. Nonetheless, we see the same trend that the reduction rule is more likely to be effective the higher the locality and heterogeneity. In the extreme regimes (bottom left or top right), we observe the same behavior as for the generated networks with relative kernel sizes close to 1 and 0, respectively, for almost all networks. Moreover, there is dichotomy in the sense that many instances are either (almost) completely solved by the dominance rule or the rule is basically inapplicable. In fact, 30.9% of the real-world networks are reduced to below 5% of their original size, while 16.3% are reduced by less than 5%.

Discussion. Though vertex cover is NP-hard [35], it is rather approachable: It can be solved in $1.1996^n n^{O(1)}$ time [47] and there is a multitude of FPT-algorithms with respect to the solution size k [23], the fastest one running in $O(1.2738^k + kn)$ [14]. This basis was improved by Harris and Narayanaswamy in a recent preprint [32] stating a running time of $O^*(1.25400^k)$ where O^* suppresses polynomial factors. Moreover, there are good practical algorithms [1, 46]. Both algorithms apply a suite of reduction rules, including the dominance rule or a generalization. We note that the dominance rule is closely related to Weihe's

reduction rules for hitting set [46]. Our previous experiments for Weihe’s reduction rules match our results: they work well if the instances are local and heterogeneous [7]. Concerning theoretic analysis on models, we know that on hyperbolic random graphs, the dominance rule is sufficiently effective to yield a polynomial time algorithm [6]. Thus, it is not surprising that the top-right corner in Figure 7 is mostly green.

We see two main directions for future research. First, concerning the dominance rule, we have seen that heterogeneity and locality are a good predictor for the effectiveness in the extreme regimes. However, there is a regime of moderate heterogeneity and locality where we see a mix of high and low effectiveness. This indicates that other properties are the deciding factor for these instances and it would be interesting to figure out these properties. The second direction is to investigate the effectiveness of other techniques for solving vertex cover depending on the network properties. This includes the study of techniques used in existing solvers [1, 46] but also the development of new techniques that are tailored towards less local or less heterogeneous instances. Specifically the algorithm of Akiba and Iwata [1] performs well on social networks (high locality and heterogeneity) but fails on road networks (low heterogeneity). Thus, techniques tailored towards solving homogeneous instances could lead to an algorithm that is more efficient on a wider range of instances.

4.4 The Louvain Algorithm for Graph Clustering

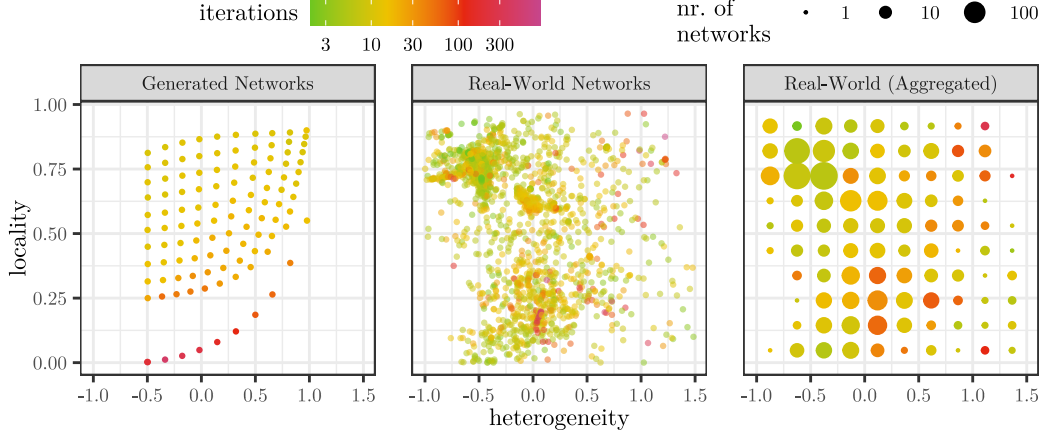
Let $V_1 \cup \dots \cup V_k = V$ be a *clustering* where each vertex set V_i is a *cluster*. One is usually interested in finding clusterings with dense clusters and few edges between clusters, which is formalized using some quality measure, e.g., the so-called modularity. A common subroutine in clustering algorithms is to apply the following local search. Start with every vertex in its own cluster. Then, check for each vertex $v \in V$ whether moving v into a neighboring cluster improves the clustering. If so, v is moved into the cluster yielding the biggest improvement. This is iterated until no improvement can be achieved. Doing this with the modularity as quality measure (and subsequently repeating it after contracting clusters) yields the well-known Louvain algorithm [4].

The run time of the Louvain algorithm is dominated by the number of iterations of the initial local search. Figure 8 shows this number of iterations. It excludes four real-world networks with more than 1 k iterations (1403, 1403, 5003, and 19983).

Impact of Locality and Heterogeneity. For the generated instances, the number of iterations is generally low but increasing when decreasing the locality. To discuss this in more detail, recall that each dot in the left plot represents the average of five networks randomly generated with the same set of parameters. Moreover, recall that the bottom-left dot represents Erdős–Rényi graphs, the rest of the bottom row represents Chung–Lu graphs and all other points represent GIRGs.

For GIRGs, the average number of iterations ranges from 9.4 to 55.4 for the different parameter configurations. Moreover, the number of iterations starts to rise only for low localities. For 83 % of the configurations the average number of iterations lies below 20. For the Erdős–Rényi graphs we obtain an average of 196.4 iterations and for Chung–Lu graphs it goes up to 443.40 for one configuration. However, these average values over five generated instances have to be taken with a grain of salt as there is a rather high variance, e.g., the number of iterations for the five Chung–Lu graphs with power-law exponent 25 ranges from 104 up to 333.

For the real-world networks there is no clear trend depending on locality or heterogeneity. In general, the number of iterations is rather low except for some outliers. While the strongest



■ **Figure 8** Number of iterations of the first local search of the Louvain algorithm. The color scale is logarithmic. Four outliers (real-world) with more than 1 k iterations are excluded.

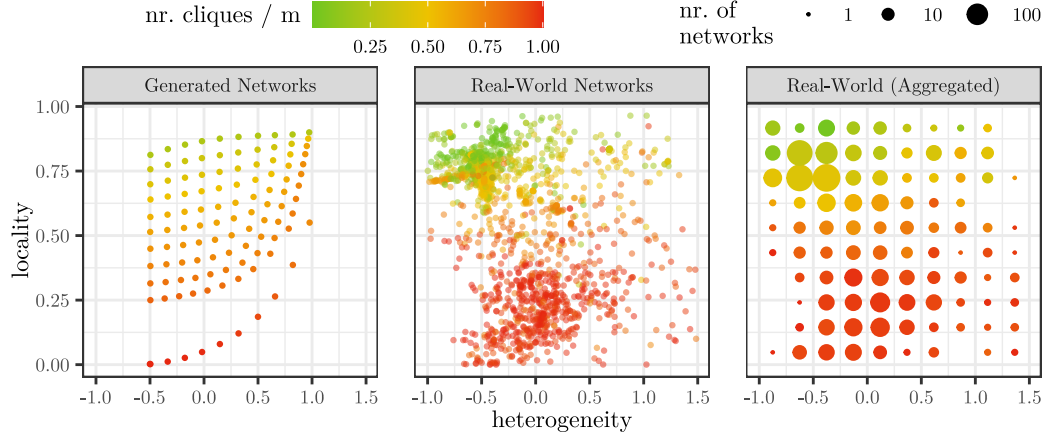
outlier requires almost 20 k iterations, 98.6 % of the networks have at most 100 iterations.

Discussion. The Louvain algorithm has been introduced by Blondel, Guillaume, Lambiotte, and Lefebvre [4]. Discussing the plethora of work building on the Louvain algorithm is beyond the scope of this paper. Concerning its running time, the worst-case number of iterations of the Louvain algorithm can be upper bounded by $O(m^2)$ due to the fact that the modularity is bounded and each vertex move improves it by at least $\Omega(1/m^2)$. Moreover, there exists a graph family that requires $\Omega(n)$ iterations for the first local search [34, Proposition 3.1]. Note that a linear number of iterations leads to a quadratic running time, which is prohibitive for larger networks.

Our experiments indicate that locality or heterogeneity are not the properties that discriminate between easy and hard instances. For generated instances, there is the trend that low locality increases the number of iterations, which does not transfer to the real-world networks (or is at least less clear). However, the general picture that most instances require few iterations while there are some outliers coincides for generated and real-world networks.

We believe that the observed behavior can be explained as follows. There are two factors that increase the number of iterations. First, one can craft very specific situations in which individual vertices move into a cluster, trigger a change there and then continue into another cluster. These specific structures are unlikely to appear in practice as well as in random instances, which is why we observe the overall low number of iterations in our experiments. The second factor increasing the number of iterations is a lack of clear community structure. A vertex that fits more or less equally well to different communities is likely to swap its cluster more often when the clustering slightly changes during the local search. This is why we see an increased number of iterations on the generated networks with low locality. This interpretation is also supported by the fact that Louvain performs provably well on the stochastic block model [19]; a network model with a very clear community structure of non-overlapping clusters.

For future research, we believe it is highly interesting to support our above interpretation with theoretical evidence. In particular, it would be interesting to understand how the local search behaves on a model with underlying geometry, which facilitates structures of overlapping communities.



■ **Figure 9** The number of maximal cliques relative to m depending on the heterogeneity and locality, restricted to networks where this value is at most 1 (93 % of the networks).

4.5 Maximal Cliques

A *clique* is a subset of vertices $C \subseteq V$ such that C induces a complete graph, i.e., any pair of vertices in C is connected. A clique is *maximal*, if it is not contained in any other clique. In the following, we are never interested in non-maximal cliques. Thus, whenever we use the term *clique*, it implicitly refers to a maximal clique. To enumerate all cliques, we used the algorithm by Eppstein, Löffler, and Strash [25], using their implementation [26, 27].

As the cliques of a network can be enumerated in polynomial time per clique [41], the number of maximal cliques is a good indicator for the hardness of an instance. To our surprise, the number of cliques does not exceed the number of edges m for all generated and most real-world networks. Out of the 2740 real-world networks, 2552 (93 %) have at most m and 187 have more than m cliques. For the remaining 1 network, the timeout of 30 min was exceeded. Figure 9 shows the number of cliques relative to m for all networks with at most m cliques.

Impact of Locality and Heterogeneity. One can see that the networks (generated and real-world) with low locality have roughly m cliques, while the number of cliques decreases for increasing locality. Moreover, among networks with locality, there is the slight trend that networks with higher heterogeneity have more cliques.

It is not surprising that networks with low locality have roughly m cliques, as graphs without triangles have exactly m cliques. For graphs with higher locality, there are two effects counteracting each other. On the one hand, multiple edges combine into larger cliques, which decreases the number of cliques. On the other hand, each edge can be contained in multiple cliques, which increases the number of cliques. Our experiments show that the former effect usually supersedes the latter, i.e., the size of the cliques increases more than the number of cliques each edge is contained in.

Discussion. There are many results on enumerating cliques and on the complementary problem of enumerating independent sets; discussing them all is beyond the scope of this paper. Here, we focus on discussing two results that are closely related. They are based on

the degeneracy and the so-called (weak) closure¹¹ of a network.

The degeneracy is a robust measure for the sparsity of a network, i.e., the degeneracy is low only if the graph does not include a dense subgraph. Eppstein, Löffler and Strash [26] give an algorithm for enumerating all cliques that runs in $O(dn3^{d/3})$ time, where d is the degeneracy. We use this algorithm for our experiments as it performs very well in practice.

Fox, Roughgarden, Seshadhri, Wei, and Wein [29] introduced the closure as a measure that captures the tendency that common neighbors facilitate direct connections, i.e., as a measure for locality. Additionally, they introduced the weak closure as a more robust measure. Fox et al. show that weakly c -closed graphs have at most $3^{(c-1)/3}n^2$ cliques. For c -closed graphs they give the additional upper bound of $4^{(c+4)(c-1)/2}n^{2-2^{1-c}}$. Together with an algorithm that takes polynomial time per clique [41], this shows that enumerating all cliques is fixed-parameter tractable with respect to the (weak) closure.

Comparing this to our empirical observations, the number of cliques is at most m for 93 % of real-world networks, while the theoretical results give exponential bounds on how much bigger than m the number cliques can be. Nonetheless, qualitatively speaking, the bounds for degeneracy and closure show that sparsity and locality lead to a low number of cliques. This matches our observations on real-world networks, i.e., most of them are sparse and have few cliques and the number of cliques decreases with increasing locality. Unfortunately, this interpretation does not withstand a closer look. To study how indicative the degeneracy and (weak) closure actually are for the number of cliques, we also computed¹² these parameters for the networks in our dataset. We then study how the number of cliques depends on these parameters as well as the relation between the parameters. As this is somewhat beyond the core focus of the paper, we only mention the main insights here. The detailed results can be found in Appendix E.

For the 93 % of networks with at most m cliques, the closure does not correlate with the number of cliques. Even worse, the weak closure and the degeneracy have a slight negative correlation, i.e., a lower parameter corresponds to a higher number of cliques. On the remaining 7 %-networks, the picture is somewhat different. While the closure is still a bad indicator for the number of cliques, the number of cliques is highly correlated with the degeneracy and the weak closure. Thus, degeneracy and weak closure provide a good measure of hardness at least for the few somewhat hard instances with more than m cliques. However, we note that degeneracy and weak closure are almost identical on these networks. Thus, weak closure is mostly a measure of sparsity rather than of locality.

To summarize, although the existing theoretical results provide valuable insights, they cannot explain the observed behavior on the majority of the networks. While providing strong upper bounds, these parameterized results suffer from the same issue that a worst-case analysis often has. The worst case is usually harder than the typical case and this does not change by restricting the set of considered instances to those with small degeneracy or closure. In contrast, our experiments show that the network models yield surprisingly accurate predictions. They predict that one should generally expect sparse networks to have at most m cliques and that the number of cliques is lower for networks with high locality. Moreover, even the slight increase with increasing heterogeneity is given for the generated as well as for the real-world networks. For future research we believe that it is highly interesting to complement our empirical findings theoretically by proving that the expected number of cliques is below m . Moreover, our findings reopen the question of finding deterministic

¹¹ For a formal definition of degeneracy and (weak) closure see the original papers or Section E.1.

¹² We give an algorithm for efficiently computing the weak closure in Section E.2.

parameters that allow to give strong bounds on the number of cliques while capturing most real-world networks.

4.6 Chromatic Number

The *chromatic number* χ of G is the smallest number of colors one can use to color the vertices of G without assigning adjacent vertices the same color. The size of any clique in G is a lower bound on the chromatic number. Thus, for the *clique number* ω of G , which is the size of the maximum clique in G , we have $\chi \geq \omega$. To compute χ , it is safe to reduce G to its ω -core, i.e., to iteratively remove all vertices with degree less than ω . After coloring the resulting *kernel* optimally, one can always color the previously removed vertices with at most ω colors [43].

The size of the kernel after applying this reduction is a good indicator for the hardness of an instance. For each network in our data set, we first compute the clique number ω by enumerating all maximal cliques as described in Section 4.5. We then compute the ω -core to obtain the kernel. Let c be the number of vertices of the kernel. Figure 10a shows the exponent x for the kernel size $c = n^x$, excluding 1 network where the clique computation exceeded the timeout of 30min. As we observed that the average degree of the generated instances has a substantial impact on the kernel size, we additionally consider generated instances with average degree 20 (instead of the usual average degree of 10).

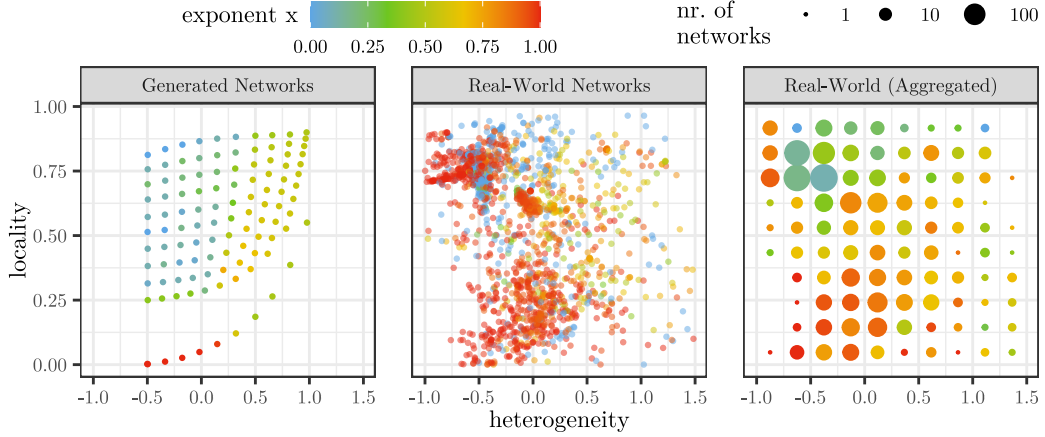
Impact of Locality and Heterogeneity. For the generated networks, one can make three main observations. First, graphs with higher locality have smaller kernels. Second, for highly heterogeneous networks, the kernel size is always moderate independent of the locality. Third, the average degree has a strong impact on the applicability of the reduction rule, with much smaller kernels for lower average degrees.

Many real-world instances are either heavily reduced or the reduction rule is almost inapplicable, yielding a very noisy picture. The noisiness indicates that locality and heterogeneity are not the only relevant factors for the kernel size. However, the overall trend is similar to the generated instances. Moreover, the noisiness is also present in the network models: The kernel size varies strongly with the average degree but even for fixed average degree we observe high variance, e.g., the exponents we get for the five generated GIRGs with average degree 20, power-law exponent 5.1 and temperature 0.76 are 0.00, 0.00, 0.99, 0.99, and 0.99.

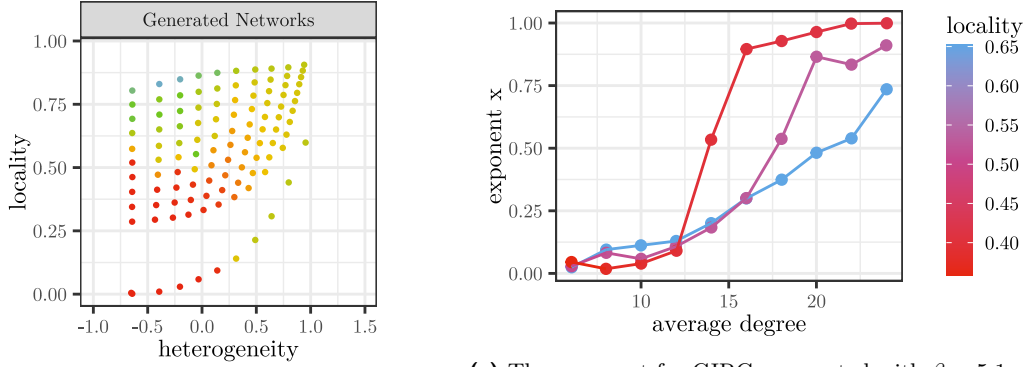
In the following, we first discuss the impact of the average degree in more detail and then offer a potential explanation for the observed variance in kernel size.

Average Degree of Generated Instances. As mentioned above, the comparison of Figures 10a and 10b shows that a higher average degree leads to larger kernels and thus harder instances. This dependence on the average degree can be seen in more detail in Figure 10c. It shows the exponent (averaged over 30 sampled instances) for GIRGs with three parameter settings depending on the average degree. For GIRGs with high temperature (low locality) we see a threshold behavior going from small kernels for low average degree to large kernels for high average degree. For lower temperatures (high locality), the transitions happens later and less steeply. This fits to the previously observed separation between difficult non-local and easy local instances, which moves up to higher locality values for an increasing average degree.

Variance in the Kernel Size – Clique Number and Degeneracy. Studying the clique number in comparison to the degeneracy yields a potential explanation for the observed



(a) Dependence of the exponent x on locality and heterogeneity. The average degree for the generated networks is 10.



(b) The same plot as in (a) but with average degree 20 instead of 10.

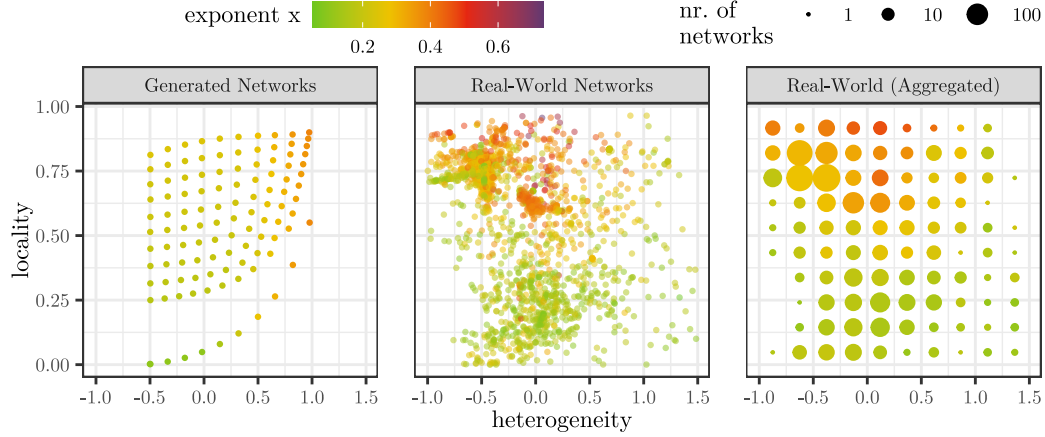
(c) The exponent for GIRGs generated with $\beta = 5.1$ and $T \in \{0.62, 0.76, 0.88\}$ depending on the average degree. Each dot represents 30 networks.

Figure 10 The exponent x of the kernel size $c = n^x$ after applying the chromatic number reduction rule.

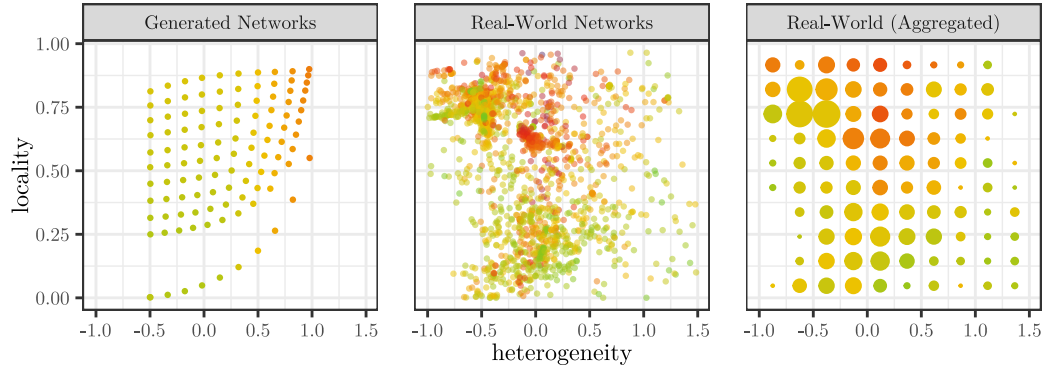
variance in the kernel size; see Figure 11.

Recall that we use the clique number ω as lower bound for the chromatic number. Thus, a larger ω yields a better lower bound, implying that the reduction rule can remove vertices of higher degree. However, the size of the kernel still depends on the structure of the remaining graph, i.e., on whether there are sufficiently many low-degree vertices that can be removed. This property is captured by the degeneracy d of the graph. In particular, note that the degeneracy is lower-bounded by $\omega - 1$. If the degeneracy is exactly $\omega - 1$, then the reduction rule completely solves the instance. If the degeneracy is higher, the kernel can be very large.

In Figure 11, we can make multiple observations. Locality and heterogeneity seem to be the core factors impacting the clique size and the degeneracy, and the dependence is similar for generated and real-world networks. However, the dependence is almost identical for clique size and degeneracy. Thus, whether $d = \omega - 1$, which yields an empty kernel or $d > \omega - 1$, yielding a non-empty kernel, often comes down to a property other than locality and heterogeneity, which explains the high variance observed above. Also observe how the difference between clique size and degeneracy is slightly higher for less local graphs, which fits to the previous observation that non-local graphs tend to have larger kernels.



(a) The exponent x of the clique number $\omega = n^x$ depending on locality and heterogeneity.



(b) The exponent x of the degeneracy $d = n^x$ depending on locality and heterogeneity.

■ **Figure 11** Comparison between the clique number and the degeneracy.

Discussion. The reduction rule we considered here has been described by Verma, Buchanan, and Butenko [43], who demonstrated that the clique number is a good lower bound for the chromatic number on real-world instances. Another lower bound method based on degree-bounded independent sets performing very well in practice has been introduced by Lin, Cai, Luo, and Su [38]. Concerning the clique number, Walteros and Buchanan [44] have shown that in many real-world networks, the *clique-core gap* $g = d + 1 - \omega$ is small, and provide an $O(m^{1.5})$ algorithm for the clique number if this gap is constant. However, they leave a potential parameterization for the chromatic number based on the clique-core gap as an open problem.

Concerning the impact of locality and heterogeneity, our results reveal a highly interesting effect. We have two characteristics (clique number and degeneracy), where locality and heterogeneity are the crucial factors. However, for an algorithm whose efficiency is essentially based on the comparison of the two characteristics, properties besides locality and heterogeneity have to tip the scale for whether the algorithm performs well or not. This is an interesting insight as this effect might pose a threat to external validity when considering more complicated algorithms based on multiple structural properties. In this specific case, however, the behavior observed on real-world instances is nonetheless quite similar to that on generated instances, including the high variance due to the above effect.

For future research, it would be interesting to study the reduction rule based on maximum cliques theoretically on the different network models. We believe that this can give a better understanding of what properties tip the scale in case the degeneracy is higher than the clique number, potentially leading to improved algorithms. This can also lead to interesting technical contributions like, e.g., understanding the potential threshold behavior when it comes to the dependence on the average degree.

5 Discussion and Conclusion

Networks from different domains have varying structural properties. Thus, trying to find probability distributions that match or closely approximate those of real-world networks seems like a hopeless endeavor. Moreover, even if we knew such a probability distribution, it would most likely be highly domain specific and too complicated for theoretical analysis.

Our View on Average-Case Analysis. A more suitable approach to average case analysis is the use of models that assume few specific structural properties and are as unbiased as possible beyond that. If the chosen properties are the dominant factors for the algorithm's performance, we obtain external validity, i.e., the results translate to real-world instances even though they do not actually follow the assumed probability distributions. There are two levels of external validity.

- The models capture the performance-relevant properties sufficiently well that algorithms perform similar on generated and real-world networks.
- The models are too much of an idealization for this direct translation to practical performance. However, varying a certain structural property in this idealized world has the same qualitative effect on performance as it has on real-world networks.

Though an average case analysis cannot yield strong performance guarantees, with the above notions of external validity, it can give insights into what properties are crucial for performance (first level) and how the performance depends on a property (second level). Moreover, even a lack of external validity can yield valuable insights in the following sense. Assume we have the hypothesis that property X is the crucial factor for algorithmic performance and thus we study a model with property X as null model. Then, a lack of external validity lets us refute the hypothesis as there clearly has to be a different property impacting the performance.

Impact of Locality and Heterogeneity. Non-surprisingly, the performance on real-world networks depending on locality and heterogeneity is more noisy compared to the generated networks, as real-world networks are diverse and vary in more than just these two properties. That being said, the observations on the models and in practice coincide almost perfectly for the bidirectional search and the enumeration of maximal cliques. For the maximal cliques, the match even includes constant factors, which is particularly surprising, as these numbers are below m while the worst case is exponential.

For the vertex cover domination rule as well as the iFUB algorithm, we obtain a slightly noisier picture. However, the overall trend matches well, which indicates that locality and heterogeneity are crucial factors for the performance, but not the only ones. For the iFUB algorithm, we already identified the existence of central vertices as additional factor (difference between torus and square as underlying geometry).

For the chromatic number, we observe that heterogeneity and locality are important but not the only factors impacting performance. Nonetheless, the performance is similar on the models compared to real-world networks.

For the Louvain clustering algorithm, the models and real-world networks coincide insofar, that the number of iterations is low, with few exceptions. This indicates that locality and heterogeneity are not the core properties for differentiating between hard and easy instances.

Conclusions. Locality and heterogeneity have significant impact on the performance of many algorithms. We believe that it is useful for the design of efficient algorithms to have these two dimensions of instance variability in mind. Moreover, GIRGs [12] with the available efficient generator [9] provide an abundance of benchmark instances on networks with varying locality and heterogeneity. Finally, we believe that average case analyses on the four extreme cases can help to theoretically underpin practical run times. The four extreme cases can, e.g., be modeled using geometric random graphs for local plus homogeneous, hyperbolic random graphs¹³ for local plus heterogeneous, Erdős-Rényi graphs for non-local plus homogeneous, and Chung-Lu graphs for non-local plus heterogeneous networks.

References

- 1 Takuya Akiba and Yoichi Iwata. Branch-and-reduce exponential/FPT algorithms in practice: A case study of vertex cover. *Theoretical Computer Science*, 609:211–225, 2016. doi:10.1016/j.tcs.2015.09.023.
- 2 Josh Alman and Virginia Vassilevska Williams. A refined laser method and faster matrix multiplication. In *ACM-SIAM Symposium on Discrete Algorithms (SODA)*, pages 522–539, 2021. doi:10.1137/1.9781611976465.32.
- 3 Albert-László Barabási and Réka Albert. Emergence of scaling in random networks. *Science*, 286(5439):509–512, 1999. doi:10.1126/science.286.5439.509.
- 4 Vincent D Blondel, Jean-Loup Guillaume, Renaud Lambiotte, and Etienne Lefebvre. Fast unfolding of communities in large networks. *Journal of Statistical Mechanics: Theory and Experiment*, 2008(10):P10008, 2008. doi:10.1088/1742-5468/2008/10/p10008.
- 5 Thomas Bläsius and Philipp Fischbeck. On the external validity of average-case analyses of graph algorithms. In *European Symposium on Algorithms (ESA)*, pages 21:1–21:14, 2022. doi:10.4230/LIPIcs.ESA.2022.21.
- 6 Thomas Bläsius, Philipp Fischbeck, Tobias Friedrich, and Maximilian Katzmann. Solving vertex cover in polynomial time on hyperbolic random graphs. *Theory of Computing Systems*, 2021. doi:10.1007/s00224-021-10062-9.
- 7 Thomas Bläsius, Philipp Fischbeck, Tobias Friedrich, and Martin Schirneck. Understanding the effectiveness of data reduction in public transportation networks. In *Workshop on Algorithms and Models for the Web-Graph (WAW)*, pages 87–101, 2019. doi:10.1007/978-3-030-25070-6_7.
- 8 Thomas Bläsius, Cedric Freiberger, Tobias Friedrich, Maximilian Katzmann, Felix Montenegro-Retana, and Marianne Thieffry. Efficient shortest paths in scale-free networks with underlying hyperbolic geometry. *ACM Transactions on Algorithms (TALG)*, 18(2):19:1–19:32, 2022. doi:10.1145/3516483.
- 9 Thomas Bläsius, Tobias Friedrich, Maximilian Katzmann, Ulrich Meyer, Manuel Penschuck, and Christopher Weyand. Efficiently generating geometric inhomogeneous and hyperbolic random graphs. In *European Symposium on Algorithms (ESA)*, pages 21:1–21:14, 2019. doi:10.4230/LIPIcs.ESA.2019.21.
- 10 Michele Borassi, Pierluigi Crescenzi, and Luca Trevisan. An axiomatic and an average-case analysis of algorithms and heuristics for metric properties of graphs. In *ACM-SIAM Symposium on Discrete Algorithms (SODA)*, pages 920–939, 2017. doi:10.1137/1.9781611974782.58.

¹³GIRGs can be seen as common generalization of geometric and hyperbolic random graphs.

- 11 Michele Borassi and Emanuele Natale. KADABRA is an ADaptive algorithm for betweenness via random approximation. *ACM Journal of Experimental Algorithmics (JEA)*, 24(1):1.2:1–1.2:35, 2019. doi:10.1145/3284359.
- 12 Karl Bringmann, Ralph Keusch, and Johannes Lengler. Geometric inhomogeneous random graphs. *Theoretical Computer Science*, 760:35–54, 2019. doi:10.1016/j.tcs.2018.08.014.
- 13 Shiri Chechik, Edith Cohen, and Haim Kaplan. Average distance queries through weighted samples in graphs and metric spaces: High scalability with tight statistical guarantees. In *International Workshop on Approximation Algorithms for Combinatorial Optimization (APPROX)*, pages 659–679, 2015. doi:10.4230/LIPIcs.APPROX-RANDOM.2015.659.
- 14 Jianer Chen, Iyad A. Kanj, and Ge Xia. Improved upper bounds for vertex cover. *Theoretical Computer Science*, 411(40-42):3736–3756, 2010. doi:10.1016/j.tcs.2010.06.026.
- 15 Markus Chimani, Carsten Gutwenger, Michael Jünger, Gunnar W. Klau, Karsten Klein, and Petra Mutzel. The open graph drawing framework (OGDF). pages 543–569. 2013.
- 16 Fan Chung and Linyuan Lu. The average distances in random graphs with given expected degrees. *Proceedings of the National Academy of Sciences*, 99(25):15879–15882, 2002. doi:10.1073/pnas.252631999.
- 17 Fan Chung and Linyuan Lu. Connected components in random graphs with given expected degree sequences. *Annals of Combinatorics*, 6(2):125–145, 2002. doi:10.1007/PL00012580.
- 18 Fan RK Chung. Diameters of graphs: Old problems and new results. *Congressus Numerantium*, 60(2):295–317, 1987.
- 19 Vincent Cohen-Addad, Adrian Kosowski, Frederik Mallmann-Trenn, and David Saulpic. On the power of Louvain in the stochastic block model. In *Conference on Neural Information Processing Systems (NeurIPS)*, 2020. URL: <https://proceedings.neurips.cc/paper/2020/hash/29a6aa8af3c942a277478a90aa4cae21-Abstract.html>.
- 20 Stephen A. Cook. The complexity of theorem-proving procedures. In *Symposium on the Theory of Computing (STOC)*, pages 151–158, 1971. doi:10.1145/800157.805047.
- 21 Pierluigi Crescenzi, Roberto Grossi, Claudio Imbrenda, Leonardo LANZI, and Andrea Marino. Finding the diameter in real-world graphs - experimentally turning a lower bound into an upper bound. In *European Symposium on Algorithms (ESA)*, pages 302–313, 2010. doi:10.1007/978-3-642-15775-2_26.
- 22 Pilu Crescenzi, Roberto Grossi, Michel Habib, Leonardo LANZI, and Andrea Marino. On computing the diameter of real-world undirected graphs. *Theoretical Computer Science*, 514:84–95, 2013. doi:10.1016/j.tcs.2012.09.018.
- 23 Marek Cygan, Fedor V. Fomin, Lukasz Kowalik, Daniel Lokshtanov, Dániel Marx, Marcin Pilipczuk, Michal Pilipczuk, and Saket Saurabh. *Parameterized Algorithms*. Springer, 2015. doi:10.1007/978-3-319-21275-3.
- 24 Derek J. de Solla Price. A general theory of bibliometric and other cumulative advantage processes. *Journal of the Association for Information Science and Technology (JASIST)*, 27(5):292–306, 1976. doi:10.1002/asi.4630270505.
- 25 David Eppstein, Maarten Löffler, and Darren Strash. Listing all maximal cliques in sparse graphs in near-optimal time. In *International Symposium on Algorithms and Computation (ISAAC)*, pages 403–414, 2010. doi:10.1007/978-3-642-17517-6_36.
- 26 David Eppstein, Maarten Löffler, and Darren Strash. Listing all maximal cliques in large sparse real-world graphs. *ACM Journal of Experimental Algorithmics (JEA)*, 18, 2013. doi:10.1145/2543629.
- 27 David Eppstein and Darren Strash. Listing all maximal cliques in large sparse real-world graphs. In *Symposium on Experimental and Efficient Algorithms (SEA)*, pages 364–375, 2011. doi:10.1007/978-3-642-20662-7_31.
- 28 P. Erdős and A. Rényi. On random graphs I. *Publicationes Mathematicae*, 6:290–297, 1959. URL: https://www.renyi.hu/~p_erdos/1959-11.pdf.

- 29 Jacob Fox, Tim Roughgarden, C. Seshadhri, Fan Wei, and Nicole Wein. Finding cliques in social networks: A new distribution-free model. *SIAM Journal on Computing*, 49(2):448–464, 2020. doi:10.1137/18M1210459.
- 30 M. R. Garey and David S. Johnson. *Computers and Intractability: A Guide to the Theory of NP-Completeness*. 1979.
- 31 Stefan Hachul and Michael Jünger. Drawing large graphs with a potential-field-based multilevel algorithm. In *International Symposium Graph Drawing and Network Visualization (GD)*, pages 285–295, 2004. doi:10.1007/978-3-540-31843-9_29.
- 32 David G. Harris and N. S. Narayanaswamy. A faster algorithm for vertex cover parameterized by solution size. *Computing Research Repository (CoRR)*, abs/2205.08022, 2022. URL: <http://arxiv.org/abs/2205.08022>.
- 33 Paul W. Holland, Kathryn Blackmond Laskey, and Samuel Leinhardt. Stochastic blockmodels: First steps. *Social Networks*, 5(2):109–137, 1983. doi:10.1016/0378-8733(83)90021-7.
- 34 Andrea Kappes. *Engineering Graph Clustering Algorithms*. PhD thesis, Karlsruhe Institute of Technology, 2015. URL: <http://digbib.ubka.uni-karlsruhe.de/volltexte/1000049269>.
- 35 Richard M. Karp. Reducibility among combinatorial problems. In *Computational Complexity Conference (CCC)*, pages 85–103, 1972. doi:10.1007/978-1-4684-2001-2_9.
- 36 Richard M. Karp. The probabilistic analysis of combinatorial optimization algorithms. In *International Congress of Mathematicians (ICM)*, volume 2, pages 1601–1609, 1983. URL: <https://www.mathunion.org/fileadmin/ICM/Proceedings/ICM1983.2/ICM1983.2.ocr.pdf>.
- 37 Dmitri Krioukov, Fragkiskos Papadopoulos, Maksim Kitsak, Amin Vahdat, and Marián Boguñá. Hyperbolic geometry of complex networks. *Phys. Rev. E*, 82:036106, 2010. doi:10.1103/PhysRevE.82.036106.
- 38 Jinkun Lin, Shaowei Cai, Chuan Luo, and Kaile Su. A reduction based method for coloring very large graphs. In *International Joint Conference on Artificial Intelligence (IJCAI)*, pages 517–523, 2017. doi:10.24963/ijcai.2017/73.
- 39 Clémence Magnien, Matthieu Latapy, and Michel Habib. Fast computation of empirically tight bounds for the diameter of massive graphs. *ACM Journal of Experimental Algorithmics (JEA)*, 13, 2008. doi:10.1145/1412228.1455266.
- 40 Ryan A. Rossi and Nesreen K. Ahmed. The network data repository with interactive graph analytics and visualization. In *AAAI Conference on Artificial Intelligence (AAAI)*, pages 4292–4293, 2015. URL: <http://www.aaai.org/ocs/index.php/AAAI/AAAI15/paper/view/9553>.
- 41 Shuji Tsukiyama, Mikio Ide, Hiromu Ariyoshi, and Isao Shirakawa. A new algorithm for generating all the maximal independent sets. *SIAM Journal on Computing*, 6(3):505–517, 1977. doi:10.1137/0206036.
- 42 Pim van der Hoorn, Gabor Lippner, and Dmitri Krioukov. Sparse maximum-entropy random graphs with a given power-law degree distribution. *Journal of Statistical Physics*, 173(3):806–844, 2018. doi:10.1007/s10955-017-1887-7.
- 43 Anurag Verma, Austin Buchanan, and Sergiy Butenko. Solving the maximum clique and vertex coloring problems on very large sparse networks. *INFORMS Journal on Computing*, 27(1):164–177, 2015. doi:10.1287/ijoc.2014.0618.
- 44 Jose L. Walteros and Austin Buchanan. Why is maximum clique often easy in practice? *Operations Research*, 68(6):1866–1895, 2020. doi:10.1287/opre.2019.1970.
- 45 Duncan J. Watts and Steven H. Strogatz. Collective dynamics of small-world networks. *Nature*, 393:440–442, 1998. doi:10.1038/30918.
- 46 Karsten Weihe. Covering trains by stations or the power of data reduction. In *Algorithms and Experiments (ALEX)*, pages 1–8, 1998.
- 47 Mingyu Xiao and Hiroshi Nagamochi. Exact algorithms for maximum independent set. *Information and Computation*, 255:126–146, 2017. doi:10.1016/j.ic.2017.06.001.

A Appendix – Overview

The appendix provides additional details and findings that divert from the core focus of the paper but are nonetheless worth mentioning. Appendix B contains additional details on the locality measure. In Appendix C, we discuss how we approximate the average distance of a graph. Appendix D contains some technical details on the randomly generated networks. Appendix E studies the number of maximal cliques depending on the degeneracy and (weak) closure parameters. Appendix F contains figures including the real-world networks with extreme heterogeneity.

The following list highlights some findings contained in the appendix that we believe are interesting in their own right.

- We describe how we can compute the locality of a graph. This in particular involves computing the detour distance quickly, which we can do exactly, using the knowledge about the bidirectional search from Section 4.1.
- To compute the locality, we also have to compute the average distance of a graph. For this, we provide an improved version of a previously known approximation algorithm [13] based on weighted sampling. Moreover, we observe that uniform sampling might be more efficient at least if the bidirectional search is fast.
- We provide an efficient algorithm for computing the weak closure of a graph.
- We give a detailed comparison of the weak closure with other measures (in particular with the degeneracy).

B Locality

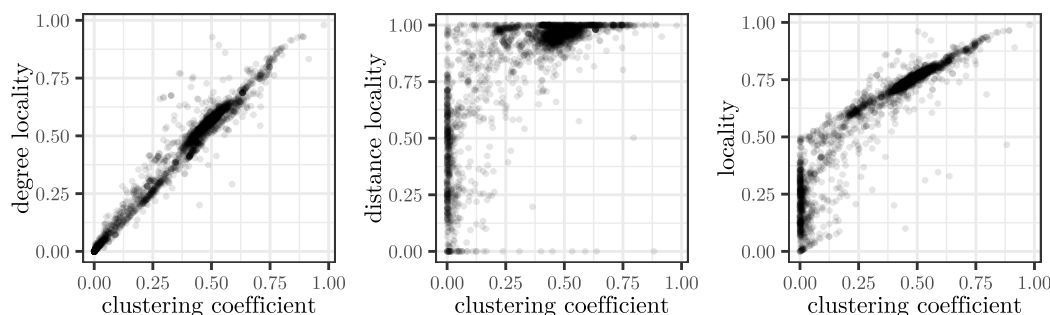
This section contains an extended discussion of our measure of locality. In Section B.1, we compare locality with the more commonly known clustering coefficient. In Section B.2, we discuss limitations of the measure. In Section B.3, we describe how we approximate the locality.

B.1 Comparison With the Clustering Coefficient

Let $G = (V, E)$ be a graph and let $v \in V$ be a vertex with $\deg(v) > 1$. Let further $G[N(v)]$ be the graph induced by v 's neighborhood $N(v)$. The *local clustering coefficient* of v is the density of $G[N(v)]$, i.e., the number of edges of $G[N(v)]$ divided by $\binom{\deg(v)}{2}$. Thus, the local clustering coefficient of v ranges between 0 if its neighborhood is an independent set and 1 if it is a clique. The *average local clustering coefficient* (or just *clustering coefficient* for short) of G is the average over all vertices with degree at least 2.¹⁴

Note that, roughly speaking, the clustering coefficient is high if the graph contains many triangles. A triangle uvw contributes the edge $\{v, w\}$ to the neighborhood of u , thereby increasing its local clustering coefficients (and symmetrically for v and w). This shows the similarity to the degree locality we introduced in Section 2.2. There, the triangle uvw makes w a common neighbor of the edge $\{u, v\}$, increasing the degree locality of $\{u, v\}$ (and symmetrically for $\{v, w\}$ and $\{w, u\}$). It is thus not surprising that the clustering coefficient and the degree locality of graphs behave very similar as can be seen in the left plot of Figure 12 (which is the same as Figure 2 but reappears here for better readability).

¹⁴Note that the local clustering coefficient is undefined for vertices of lower degree as we divide by $\binom{\deg(v)}{2} = 0$ if $\deg(v) \leq 1$.



■ **Figure 12** Comparison of the average local clustering coefficient to the degree locality (left), the distance locality (center), and the locality (right). Each dot represents one network from our data set of real-world networks.

The main disadvantage of the clustering coefficient (and of the degree locality for that matter) is that some types of graphs we would regard as highly local get very small values. An extreme case are bipartite graphs that have no triangles and thus clustering coefficient and degree locality 0. However, we would regard, e.g., grids as highly local. The goal of bringing the distance locality into the mix was to get a more fine-grained view on these networks with few triangles while keeping a measure similar to the clustering coefficient for networks with many triangles.

In the middle plot of Figure 12, we can see that the networks with low clustering coefficients yield a wide range of distance locality values. Moreover, most networks with higher clustering coefficient have distance locality close to 1. This should not come as a surprise as the distance locality of an edge is 1 for every edge contained in a triangle.

Averaging the degree and distance locality yields the locality, which is compared to the clustering coefficient in the right plot of Figure 12. This plot shows that our measure of locality achieved what we hoped for. For networks with high clustering it behaves similar to the clustering coefficient, but scaled to the interval $[0.5, 1]$. Moreover, graphs with clustering coefficient close to 0 are mapped to lower localities in the $[0, 0.5]$ range, yielding a more fine-grained perspective for those networks.

Note that the above mentioned example of a grid has a locality close to 0.5. If $G = (V, E)$ is a $\sqrt{n} \times \sqrt{n}$ -grid, then every edge $\{u, v\} \in E$ has detour distance 3 while the average distance of non-adjacent vertex pairs grows with growing n . This yields a distance locality that converges to 1 for $n \rightarrow \infty$.

B.2 Limitations

Our definition of locality has three limitations. We mentioned them earlier in Section 3 but want to discuss them here in more detail.

The first limitation is that the locality is not defined for trees. In a tree, every edge is a bridge but the distance and edge locality are only defined for non-bridge edges. However, we do not see this as a real issue as the concept of locality does not really make sense for trees anyways.

The second limitation is that distance locality is not defined for cliques. In a clique, there are no non-edges and thus the looking at the average non-edge distance does not make sense.

As already mentioned in Section 3, we circumvent these first two limitations by removing trees and dense graphs. We note that trees are not very interesting in the context of this

■ **Table 1** The networks with (uncapped) distance locality below -0.1 or average non-edge distances 2. The columns are the number of vertices n , number of edges m , the average distance $\text{dist}(E \cup \bar{E})$, the average non-edge distance $\text{dist}(\bar{E})$, the average detour distance $\text{dist}^+(E')$ of non-bridges E' , the (uncapped) distance locality $L_{\text{dist}}(G)$ of G , and the degree locality $L_{\text{deg}}(G)$.

graph	n	m	$\text{dist}(E \cup \bar{E})$	$\text{dist}(\bar{E})$	$\text{dist}^+(E')$	$L_{\text{dist}}(G)$	$L_{\text{deg}}(G)$
Chebyshev1	261	1542	1.95	2.00	2.00	0.00	0.93
fs_541_1	541	2466	1.98	2.00	2.00	0.00	0.62
lp_d6cube	6184	37 681	2.00	2.00	2.00	0.00	0.66
lp_fit2d	10 524	129 040	2.00	2.00	2.16	-116.88	0.15
bibd_17_8	24 310	680 232	2.00	2.00	2.01	-0.53	0.40
lp_fit1d	1049	13 426	1.98	2.01	2.14	-17.96	0.13
arc130	130	715	1.98	2.07	2.15	-1.18	0.69
air02	6774	61 529	2.19	2.19	2.35	-0.81	0.17
rt_lolgop	9765	10 075	2.23	2.23	2.40	-0.78	0.54
nwl4	123 409	904 906	2.31	2.31	2.94	-2.07	0.01
rt_occupywallstnyc	3609	3830	2.37	2.37	2.53	-0.42	0.41
blockqp1	60 012	300 011	2.44	2.44	2.67	-0.51	0.20
stat96v4	63 076	491 329	2.47	2.47	2.56	-0.18	0.13
bibd_9_3	84	249	2.56	2.68	2.86	-0.27	0.06
rt_barackobama	9631	9772	2.84	2.84	3.37	-0.64	0.15
n3c5-b4	252	1165	2.84	2.91	3.02	-0.12	0.01
rt_onedirection	7987	8100	2.91	2.91	3.25	-0.36	0.09
lp_standmps	1274	3878	2.98	2.99	3.10	-0.12	0.05
lp_afiro	51	100	2.88	3.04	3.16	-0.12	0.12
lp_standata	1274	3230	3.09	3.09	3.28	-0.17	0.00
primagaz	10 836	20 116	3.27	3.27	3.77	-0.39	0.00
lp_sc50a	77	155	3.25	3.38	3.59	-0.16	0.01
lp_sc50b	76	143	3.38	3.51	3.78	-0.18	0.02
lpi_ex72a	215	463	3.94	4.00	4.24	-0.12	0.01
lpi_woodinfe	89	138	4.12	4.24	4.76	-0.24	0.11
ENZYMES123	90	127	6.13	6.29	7.00	-0.16	0.15
ENZYMES	125	141	12.94	13.16	17.49	-0.39	0.01
NCI1	106	107	13.04	13.28	17.57	-0.38	0.00
FRANKENSTEIN	214	217	22.25	22.46	40.08	-0.86	0.00
pivtol	102	103	25.50	26.01	97.15	-2.96	0.02
odepa400	400	402	99.75	100.25	391.10	-2.96	0.01

paper and dense graphs are out of scope.

The third limitation is less clear-cut but also concerns the average non-edge distance $\text{dist}(\bar{E})$ in the definition of distance locality. As mentioned before, it can happen that $\text{dist}(\bar{E}) = 2$, e.g., for a wheel graph. In this case we formally defined $L_{\text{dist}}(\{u, v\}) = 0$. However, there is also already an issue if $\text{dist}(\bar{E})$ is only slightly greater than 2. In this case, the distance locality is rather volatile, yielding negative values without much meaning. This issue is increased by the fact that we approximate the average distances. Generally, the distance locality seems not the best measure for locality in the regime where it is negative.

We circumvent this issue by capping the distance locality of graphs at 0, as mentioned in Section 2.2. We note, however, that this happens only rarely. Out of all networks, the uncapped distance locality is negative for only 43 networks. Moreover, the average non-edge distance is 2 for 3 additional networks. In Table 1, we list all networks with average non-edge distance 2 and all networks with distance locality below -0.1 . Note that there are two types of instances where this appears. The instances at the top of the table have low average distances, which makes the distance locality non-robust. The instances at the bottom are close to trees with few long cycles, which yields large detour distances.

B.3 Computing the Locality

In our implementation, we compute three aggregated values; the average degree locality $L_{\deg}(G)$ of the graph G , the average detour distance $\text{dist}^+(E')$ of all non-bridges E' , and the average distance $\text{dist}(E \cup \bar{E})$ of all vertex pairs (recall that $\bar{E} = \binom{V}{2} \setminus E$). In the following, we first discuss how we compute these values and then prove some lemmas that show how these three values suffice to compute the locality $L(G)$ of G .

Computing the degree locality $L_{\deg}(G)$ in time $O(\sum_{v \in V} (\deg(v))^2)$ is more or less straight forward (very similar to computing the clustering coefficient). This yields run times that are feasible for all networks in our data set.

For the average detour distance $\text{dist}^+(E')$ of all non-bridges E' , we generally have to compute a shortest path for a linear number of start–destination pairs. Though this appears to require quadratic running time, which would be infeasible, we can make use of the following win–win situation. We know that the bidirectional search is sublinear unless the network is homogeneous and local; see Section 4.1. Moreover, if the network is homogeneous and local, the detour distances are short and thus the shortest path search can terminate after few steps. Thus, just running the bidirectional search for each non-bridge edge E' is efficient for all networks.

The straight-forward way of computing the average distance $\text{dist}(E \cup \bar{E})$ of all vertex pairs is to run a BFS from every vertex. As this is infeasible for the larger networks, we instead only approximate the average distance. Details on that can be found in Section C.

The following lemma states how we can compute the distance locality of the graph from the average detour distance $\text{dist}^+(E')$ of all non-bridges E' and the average distance $\text{dist}(\bar{E})$ of non-edges \bar{E} .

► **Lemma 1.** *The average distance locality $L_{\text{dist}}(G)$ is*

$$L_{\text{dist}}(G) = \max \left\{ 1 - \frac{\text{dist}^+(E') - 2}{\text{dist}(\bar{E}) - 2}, 0 \right\}.$$

Proof. First recall from Section 2.2 that the maximum with 0 is part of the definition of $L_{\text{dist}}(G)$. Beyond that, we have to show that computing the distance locality of a single edge based on its detour distance commutes with taking the average over all non-bridge edges. We obtain

$$\begin{aligned} L_{\text{dist}}(G) &= \frac{1}{m'} \sum_{\{u,v\} \in E'} L_{\text{dist}}(\{u,v\}) \\ &= \frac{1}{m'} \sum_{\{u,v\} \in E'} \left(1 - \frac{\text{dist}^+(u,v) - 2}{\text{dist}(\bar{E}) - 2} \right) \\ &= 1 - \frac{1}{m'} \sum_{\{u,v\} \in E'} \frac{\text{dist}^+(u,v) - 2}{\text{dist}(\bar{E}) - 2} \\ &= 1 - \frac{\frac{1}{m'} \sum_{\{u,v\} \in E'} \text{dist}^+(u,v) - 2}{\text{dist}(\bar{E}) - 2} \\ &= 1 - \frac{\text{dist}^+(E') - 2}{\text{dist}(\bar{E}) - 2}. \end{aligned}$$

◀

Finally, the following lemma shows how we can derive the average distance $\text{dist}(\bar{E})$ of non-edges \bar{E} with $\bar{m} = |\bar{E}|$ from the average distance $\text{dist}(E \cup \bar{E})$ of all vertex pairs.

► **Lemma 2.** *The average distance $\text{dist}(\overline{E})$ between non-edges is*

$$\text{dist}(\overline{E}) = \text{dist}(E \cup \overline{E}) + \frac{m}{\overline{m}}(\text{dist}(E \cup \overline{E}) - 1).$$

Proof. It holds that

$$\begin{aligned} \text{dist}(\overline{E}) &= \frac{1}{\overline{m}} \sum_{\{u,v\} \in \overline{E}} \text{dist}(u, v) \\ &= \frac{1}{\overline{m}} \left(\sum_{\{u,v\} \in \overline{E}} \text{dist}(u, v) + \sum_{\{u,v\} \in E} \text{dist}(u, v) - \sum_{\{u,v\} \in E} \text{dist}(u, v) \right) \\ &= \frac{1}{\overline{m}} \sum_{\{u,v\} \in E \cup \overline{E}} \text{dist}(u, v) - \frac{1}{\overline{m}} \sum_{\{u,v\} \in E} \text{dist}(u, v) \\ &= \frac{m + \overline{m}}{\overline{m}} \text{dist}(E \cup \overline{E}) - \frac{m}{\overline{m}} \\ &= \text{dist}(E \cup \overline{E}) + \frac{m}{\overline{m}}(\text{dist}(E \cup \overline{E}) - 1). \end{aligned}$$

◀

C Approximating Average Distances

To approximate the average distance of a graph, we implemented the algorithm by Chechik, Cohen, and Kaplan [13]; with a small improvement that is discussed in Section C.1. For a parameter k , it computes the BFS trees from roughly k vertices. We used $k = 400$ for all graphs.

To evaluate how good the approximation is, we selected eight networks with roughly 10k vertices and ran the algorithm 50 times on each of them; see Table 2. We measure the quality of the approximation using the *relative error*, which is defined as follows. Let G be a graph with (exact) average distance d and let d' be the approximation computed by the algorithm. Then the relative error is $|d - d'|/d$. Table 2 shows that the relative errors are low. Also note that the networks were selected to have varying values of locality and heterogeneity. Specifically, the first two networks are local and homogeneous, the next two are local and heterogeneous, the fifth and sixth are non-local and homogeneous, and the last two are non-local and heterogeneous.

In the remainder of this section, we want to discuss two aspects of computing the average distances that are besides the point of this paper but nonetheless interesting in their own right. First, there is a simple way to improve the approximation quality of the algorithm by Chechik, Cohen, and Kaplan [13], which we describe in Section C.1. Moreover, in Section C.2, we compare the algorithm to just sampling vertex-pairs uniformly.

C.1 Improved Approximation Quality

Given a graph $G = (V, E)$ and a parameter k , the algorithm by Chechik, Cohen, and Kaplan [13] works roughly as follows. It first computes a probability p_v for each vertex $v \in V$ such that the sum of all probabilities is in $O(k)$. Then, a sample $S \subseteq V$ is created by including v in S with probability p_v , independently of the other vertices. Note that S has expected size $\mathbb{E}[|S|] \in O(k)$. Finally, for each vertex $u \in S$, a BFS from u is run, summing the distances from u to other vertices, scaled with the factor $1/p_u$ to accommodate for the fact that u was chosen as sample with probability p_u .

■ **Table 2** The result of 50 runs of approximating the average distance with weighted sampling using $k = 400$ samples (in expectation) in each run. The columns are the number of vertices (n) and edges (m), the locality (loc) and heterogeneity (het), the exact average distance (avg dist), the smallest (min) and largest (max) estimated average distance among the 50 runs, and the median relative error (error) over the 50 runs.

graph	n	m	loc	het	avg dist	min	max	error
crack	10 240	30 380	0.77	−0.50	41.00	40.48	41.68	0.44 %
inlet	11 730	220 296	0.82	−0.56	33.81	33.24	34.60	0.38 %
sofb-Columbia2	11 706	444 295	0.61	0.05	2.84	2.81	2.86	0.33 %
ca-HepPh	11 203	117 618	0.90	0.36	4.67	4.63	4.71	0.21 %
sinc15	11 532	564 607	0.10	−0.38	3.05	3.00	3.08	0.43 %
fd15	11 532	44 206	0.30	−0.58	6.02	5.96	6.10	0.37 %
escorts	10 106	39 016	0.24	0.26	4.20	4.18	4.24	0.29 %
air03	10 757	91 006	0.13	0.83	2.46	2.44	2.48	0.21 %

Our improvement is the following. Once we have sampled the set S , we know how large S actually is. Thus, we can condition on the size of S when looking at the probability that u was chosen as a sample. Formally, after sampling S , we set $p'_u = p_u \cdot |S|/\mathbb{E}[|S|]$, which is the probability that $u \in S$ conditioned on the size of S . Then, when summing the distances from u to other vertices, we scale these distances with $1/p'_u$ instead of with $1/p_u$.

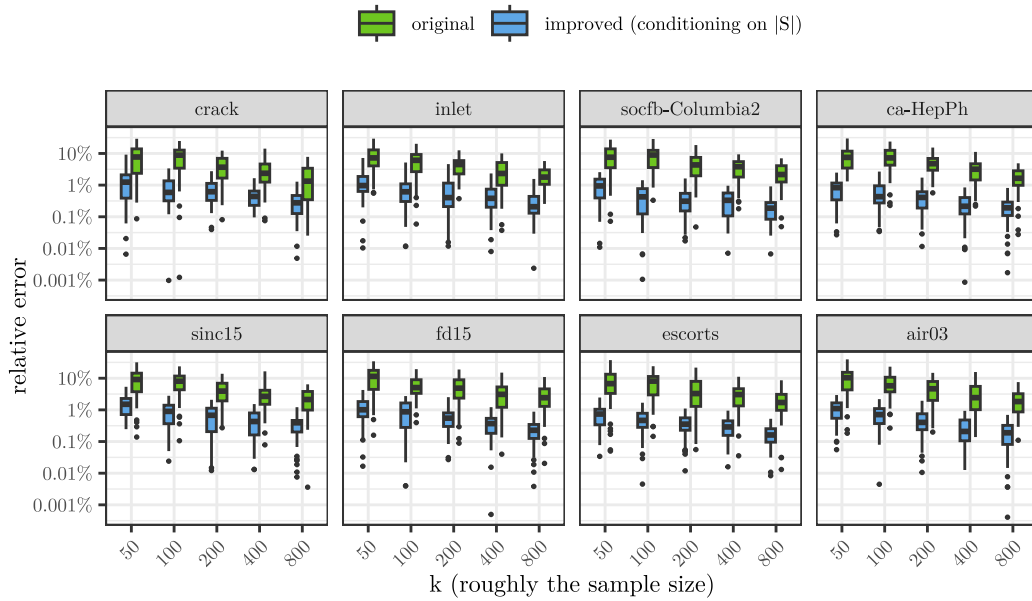
To evaluate this change, we ran both variants of the algorithm (with and without conditioning on the size of $|S|$) for different values of k on the instances in Table 2. We ran each configuration 50 times. The resulting relative errors are shown in Figure 13. Note that the our improved variant conditioning on the size of S yields a substantially better approximation.

C.2 Uniform vs. Weighted Sampling

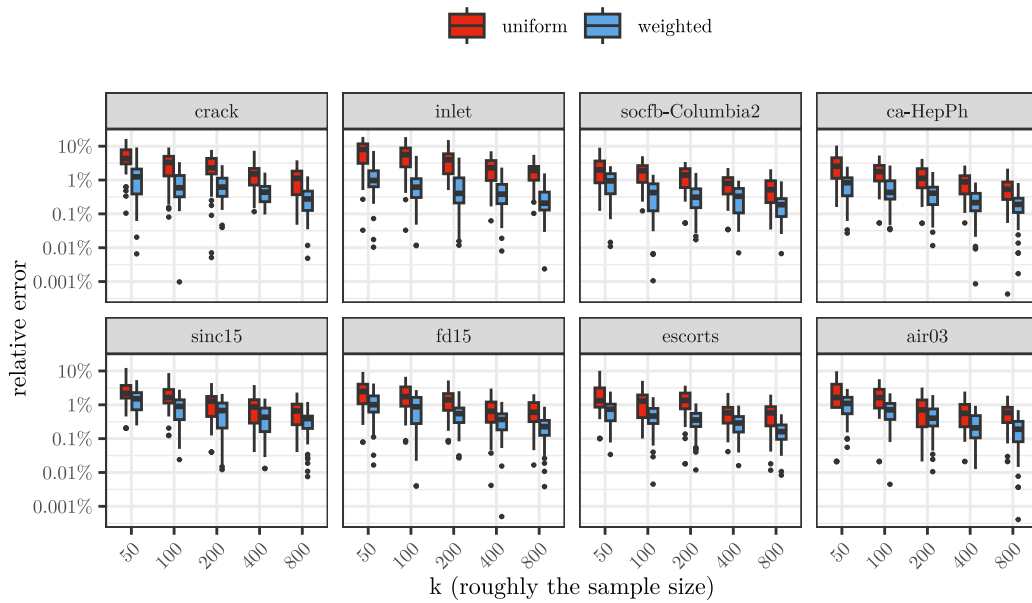
In this section, we want to compare the above algorithm with the most straight-forward method of approximating the average distance: averaging over the distance between k uniformly and independently sampled vertex pairs. In the following, we refer to this as *uniform sampling*. Moreover, we refer to the algorithm from [13] with our improvement described in the previous section as *weighted sampling*. Figure 14 shows a comparison of the average errors of uniform and weighted sampling depending on the parameter k .¹⁵ One can see that the weighted sampling performs better, which is the expected outcome.

However, this has to be taken with a grain of salt, as weighted sampling runs a full BFS for every sampled vertex, while uniform sampling only computes the shortest path between the sampled vertex pairs. While both take linear time per sample in the worst case, we know that the bidirectional BFS can compute shortest paths substantially quicker on many networks; see Section 4.1. To make a more fair comparison, we additionally ran the uniform sampling for up to $k = 6400$ vertex pairs and compare the relative errors of uniform and weighted sampling with respect to running time in Figure 15. Given our knowledge from Section 4.1, it is not surprising to see that weighted sampling is preferable over uniform sampling on the two networks with high locality and low heterogeneity, as the bidirectional search is not much faster than running a full BFS for these networks. For the other networks, however, doing the weighted sampling for more samples yields comparable, if not better,

¹⁵Note that for the weighted sampling, the expected size of S is in $O(k)$ but not exactly k . In our experiments, $|S|$ was on average $1.19 \cdot k$. Uniform sampling uses exactly k samples.



■ **Figure 13** Relative error depending on the parameter k , which roughly corresponds to the number of samples $|S|$. Each box corresponds to 50 runs. Green boxes show errors for the original algorithm as proposed by Chechik, Cohen, and Kaplan [13]. Blue boxes show errors after our adjustment of conditioning on $|S|$. Note that both axes are logarithmic.



■ **Figure 14** Relative errors depending on the parameter k . Each box corresponds to 50 runs. Red and blue boxes show errors for uniform and weighted sampling, respectively. Note that both axes are logarithmic.

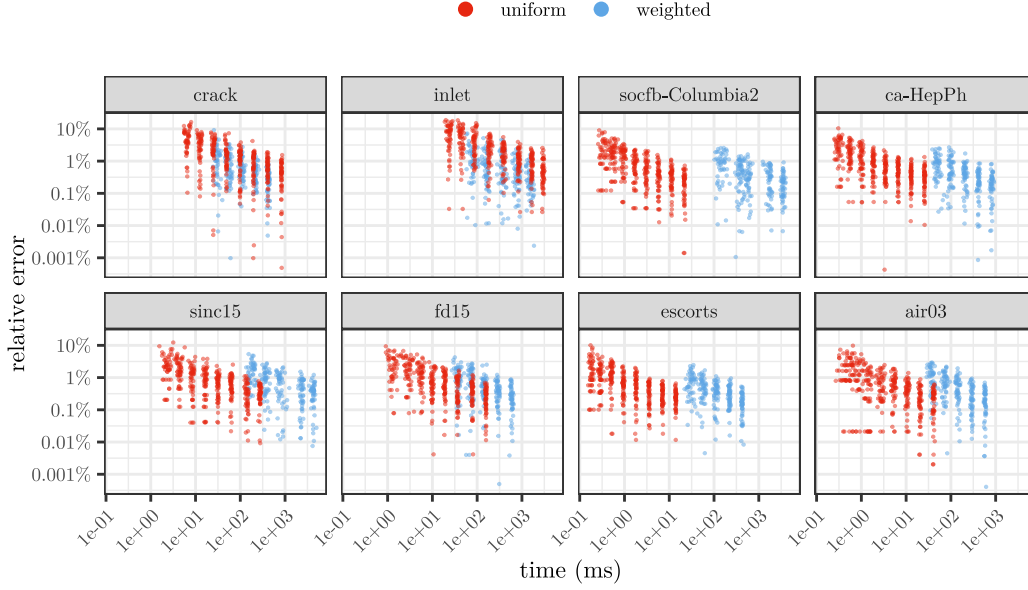


Figure 15 Relative errors depending on the run time. The parameter k determining the sample size ranges from 50 to 800 for the weighted sampling and from 50 to 6400 for the uniform sampling. The plot shows 50 runs for each value of k . Note that both axes are logarithmic.

approximations in less time.

This suggests the conclusion that one should use the weighted sampling on graphs that are local and uniform, while the uniform sampling is preferable on all other networks. To cement this conclusion, more thorough experiments would be necessary, which is beyond the scope of this paper.

D Technical Details Concerning Random Networks

In Section D.1, we observe that reducing the generated graphs to their largest connected components does not change the graph size by too much. In Section D.2 we discuss how we generate GIRGs with square as ground space, instead of the usual torus.

D.1 Giant Component

The generated graphs are not necessarily connected. Thus, as we reduce all networks to their largest connected component, the resulting graphs do not necessarily have $n = 50$ k vertices. However, the average degree of 10 is sufficiently large, so that the largest connected component is not too much smaller. Among the 500 generated GIRGs, the smallest graph has still 45 771 vertices, with an average of 49.5 k vertices. For the Chung–Lu graphs, the minimum is 45 389 and the average 49.2 k. For Erdős–Rényi, the minimum is already 49 994. Moreover, the average degrees of all generated networks are close to 10.

D.2 GIRGs With Square as Ground Space

Recall that the GIRG model uses a torus as ground space. Note that the torus is completely symmetric in the sense that every point can be treated the same. In contrast, if using a

square (or hypercube in higher dimensions) as ground space, there are special cases for points closer to the boundary of the square, which complicates theoretical analysis. For reasons described in Section 4.2, the ground space makes a difference for the diameter computation. Here we describe how we used the GIRG generator, which usually works with the torus, to generate GIRGs with unit square as ground space (still using the maximum norm).

Recall that the d -dimensional torus $\mathbb{T}^d = [0, 1]^d$ behaves like the d -dimensional cube except that distances wrap around the boundaries in each dimension. Thus, when restricting \mathbb{T}^d to points in $[0, 0.5]^d$, the distances within this part of the torus behave exactly as distances in a d -dimensional cube. We use this to generate GIRGs with a d -dimensional hypercube as follows. The generator first samples a point in $[0, 1]^d$ for each vertex. Before sampling the edges based on these vertex positions, we scale all coordinates by 0.5, yielding points in $[0, 0.5]^d$. To accommodate for the fact that this leads to smaller distances, we scale the vertex weights by 0.5^d . Afterwards, we generate the edges as for the torus [9].

To see that scaling all weights by 0.5^d achieves roughly the right average degree, recall that the probability for two vertices u and v to be connected is

$$p_{u,v} = \min \left\{ \left(\frac{1}{\|\mathbf{u} - \mathbf{v}\|^d} \cdot \frac{w_u w_v}{W} \right)^{\frac{1}{\alpha}}, 1 \right\}.$$

Note that scaling all weights by 0.5^d increases $w_u w_v$ by 0.5^{2d} and the sum of all weights W by 0.5^d , which yields a total increase of 0.5^d contributed by the weights. Moreover, scaling all coordinates by 0.5 decreases most distances by a factor of 0.5, which cancels out with the 0.5^d coming from the weights. Note that not all distances are actually scaled by 0.5: If the geodesic between \mathbf{u} and \mathbf{v} wraps around the torus, then the distance between them might actually be increased due to the scaling. However, in the context of GIRGs, this is only relevant for a sublinear fraction of vertex pairs and is thus not too relevant. Moreover, by just scaling the weights we also ignore the minimum in the formula of $p_{u,v}$. However, the deviation from the desired average degree was not too big, as we report in the following.

Among the 500 generated GIRGs with square as ground space, the smallest graph still has 45 468 vertices, with an average of 49.3k vertices. The average degrees are slightly below the target value, ranging from 8.99 to 10.24 with an average of 9.56.

E Maximal Cliques, Degeneracy, and (Weak) Closure

In this section we provide additional experiments on the number of maximal cliques in the context of degeneracy and (weak) closure. Section E.1 gives a formal definition of these parameters. In Section E.2 we provide an algorithm for efficiently computing the weak closure, which might be interesting in its own right. In Section E.3 we discuss the dependence of the number of cliques on the parameters. In Section E.4 we study how the parameters relate to each other.

E.1 Degeneracy and (Weak) Closure

The *degeneracy* d of a network is the smallest number such that iteratively removing vertices of degree at most d eliminates the whole graph.

A network is *c-closed* if every pair of vertices with at least c common neighbors is connected. Note that a single pair of vertices with many common neighbors already leads to a high closure. The weak closure addresses this issue as follows. A pair of non-adjacent vertices is a *c-bad pair* if they have at least c common neighbors. We call a vertex *c-bad* if it

appears in a c -bad pair. Otherwise, we call it c -good. A graph is *weakly c -closed* if iteratively removing c -good vertices eliminates the whole graph. Note that a c -closed graph is also weakly c -closed.

Also note the similarity between weak closure and degeneracy. Both are defined via an elimination order on the vertices. Moreover, a vertex v can have at most $\deg(v)$ common neighbors with another vertex. Thus, for a weakly c -closed graph with degeneracy d it holds that $c - 1 \leq d$.

E.2 Computing the Weak Closure

Before we describe how we compute the weak closure, note that the closure can be computed as follows. For every vertex v , look at the first two layers of the BFS-tree from v and for each node w in the second layer, count the number of length-2 paths from v to w . The node v is c -good if this count is strictly lower than c for all vertices w in the second layer. Moreover, the graph is c -closed if all vertices are c -good. The running time for each vertex is dominated by the sum of degrees of vertices in the first layer of the BFS-tree. Overall, every vertex v appears $\deg(v)$ times in the first layer, yielding a running time of $O(\sum_{v \in V} \deg^2(v))$. This is sufficiently fast for all networks in our data set.

A naive approach to compute the weak closure is as follows. Start with $c = 1$. Then run the above procedure to find the minimum value c' such that there exists a c' -good vertex. If $c < c'$, set $c = c'$ and then remove all c -good vertices. Repeat this until the graph is completely eliminated. The graph is then weakly c -closed for the final value of c . Though this is fast for many networks, it is prohibitively slow for some. In the following, we describe how to improve the running time at the cost of a higher memory consumption. Afterwards, we discuss how to decrease the memory footprint to a reasonable level.

For every vertex v , we have a priority queue Q_v that contains all vertices of distance two from v . For such a vertex w , the priority is set to the number of common neighbors of v and w , i.e., a priority of $c_{v,w}$ indicates that v and w form a $c_{v,w}$ -bad pair. Let c_v be the largest priority in Q_v . Note that, v is c_v -bad but $(c_v + 1)$ -good. Thus, we want to iteratively remove the vertex v with minimum c_v . To this end, we maintain one additional priority queue Q containing all vertices, using c_v as priority for v .

When removing a vertex u , we have to update the neighbors of u , as they lose u as common neighbor. This is done as follows. Let v and w be two neighbors of u that are not connected by an edge. Recall that the queue Q_v contains w with the priority $c_{v,w}$ indicating the number of common neighbors of v and w . As they lost u as common neighbor, we have to decrease this priority in Q_v by 1. If this decreases c_v , i.e., the maximum priority in Q_v , we also have to adapt the priority of v in the queue Q accordingly.

This algorithm takes $O(\sum_{v \in V} \deg^2(v))$ time to initialize the data structures. Moreover, when removing vertex u , we have to update $\deg^2(u)$ neighbor pairs. Assuming all queue-operations take constant time,¹⁶ this takes overall $O(\sum_{v \in V} \deg^2(v))$ time. Unfortunately, it also requires that amount of memory, which is prohibitive for some instances.

To improve the memory consumption, we make use of the following observation. Taking the squares of the degrees is particularly bad if the graph contains vertices of high degree. A vertex of high degree is responsible for many pairs of vertices that have distance 2. However, most of these pairs do not have many common neighbors, and thus will never be a c -bad

¹⁶This can be achieved using a bucket heap that makes use of the fact that the range of possible integer priorities is bounded.

pair for a relevant value of c . To phrase it differently, if we want to show that the graph is weakly c -closed, we can ignore all distance-2 pairs $v, w \in V$ that have fewer than c common neighbors. Thus, using the above notation for the queues, we do not have to insert w in the queue Q_v if $c_{v,w} < c$.

Thus, we start with the guess that the given graph is \bar{c} -closed for some value \bar{c} . Then, we compute the elimination order as above, but in the initialization of the data structures, we ignore all pairs with fewer than \bar{c} common neighbors. Assume the procedure concludes that the graph is c -closed, i.e., all vertices were c -good at the time of removal, but some $(c - 1)$ -bad vertices had to be removed. If $c \geq \bar{c}$, then the ignored vertex pairs have fewer than c common neighbors. Thus, none of these vertex pairs turns a c -good vertex into a c -bad vertex, implying that the result is correct despite ignoring some vertex pairs. On the other hand, if $c < \bar{c}$, we may have ignored some crucial pairs and have to rerun the procedure with lower \bar{c} .

Preliminary experiments showed that guessing \bar{c} even slightly too low can lead to high memory consumption, while guessing \bar{c} too high is computationally not very expensive. Starting with $\bar{c} = 30$ and successively decreasing it by 1 if necessary yields acceptable¹⁷ running times and memory footprints for all instances in our data set.

E.3 Impact of Degeneracy and Closure on the Number of Cliques

Figure 16 and Figure 17 show a pairwise comparison of degeneracy, weak closure, closure, heterogeneity, locality, and number of cliques (relative to m) for all networks with at most m cliques and more than m cliques, respectively. The bottom row and the right-most column compare the number of cliques with the other parameters.

E.3.1 Networks With at Most m Cliques.

In Figure 9, we already saw that the number of cliques increases for decreasing locality and we saw a slight increase for increasing heterogeneity. This matches to what we observe here: a strong negative correlation to the locality and a weaker positive correlation to the heterogeneity.

For degeneracy and (weak) closure, theoretical results show that low values for these parameters guarantee a low number of cliques [26, 29]. Though these theoretical bounds operate in a completely different regime (above m by factors exponential in the parameter, not below m), one could nonetheless hope that these parameters serve as a good measure for the hardness of an instance, i.e., that the number of cliques positively correlates with them. Figure 16 shows that this hope is not justified. There is little to no correlation with the closure and even a slightly negative correlation with degeneracy and weak closure.

E.3.2 Networks With More Than m Cliques.

For the networks with more than m cliques (Figure 17), one can see a strong positive correlation of the number of cliques with the degeneracy and the weak closure. Thus, for these fewer somewhat hard instances, the degeneracy and weak closure serve as good measures for how hard an instance actually is. This qualitatively matches the theoretical bounds of

¹⁷We note that there is probably still plenty room for fine-tuning. However, this is beyond the scope of this paper.

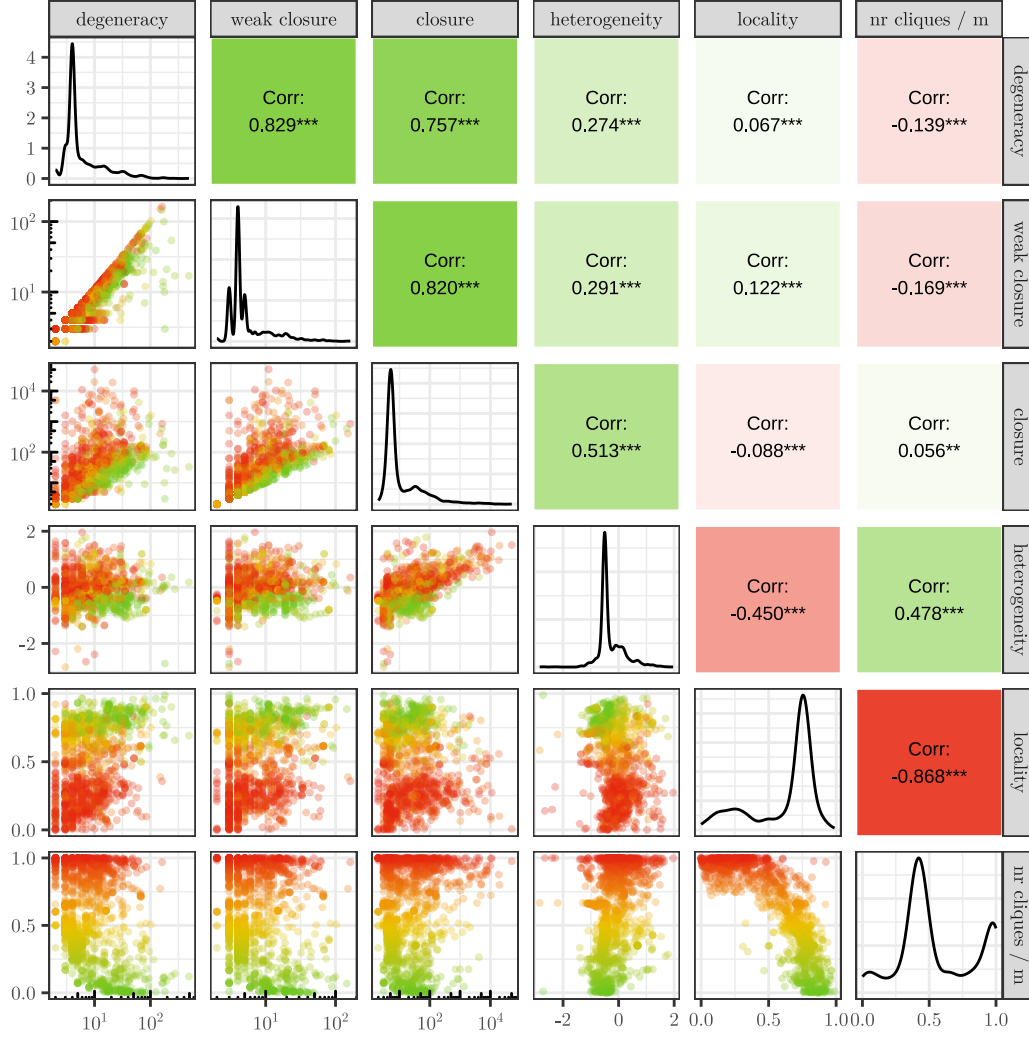
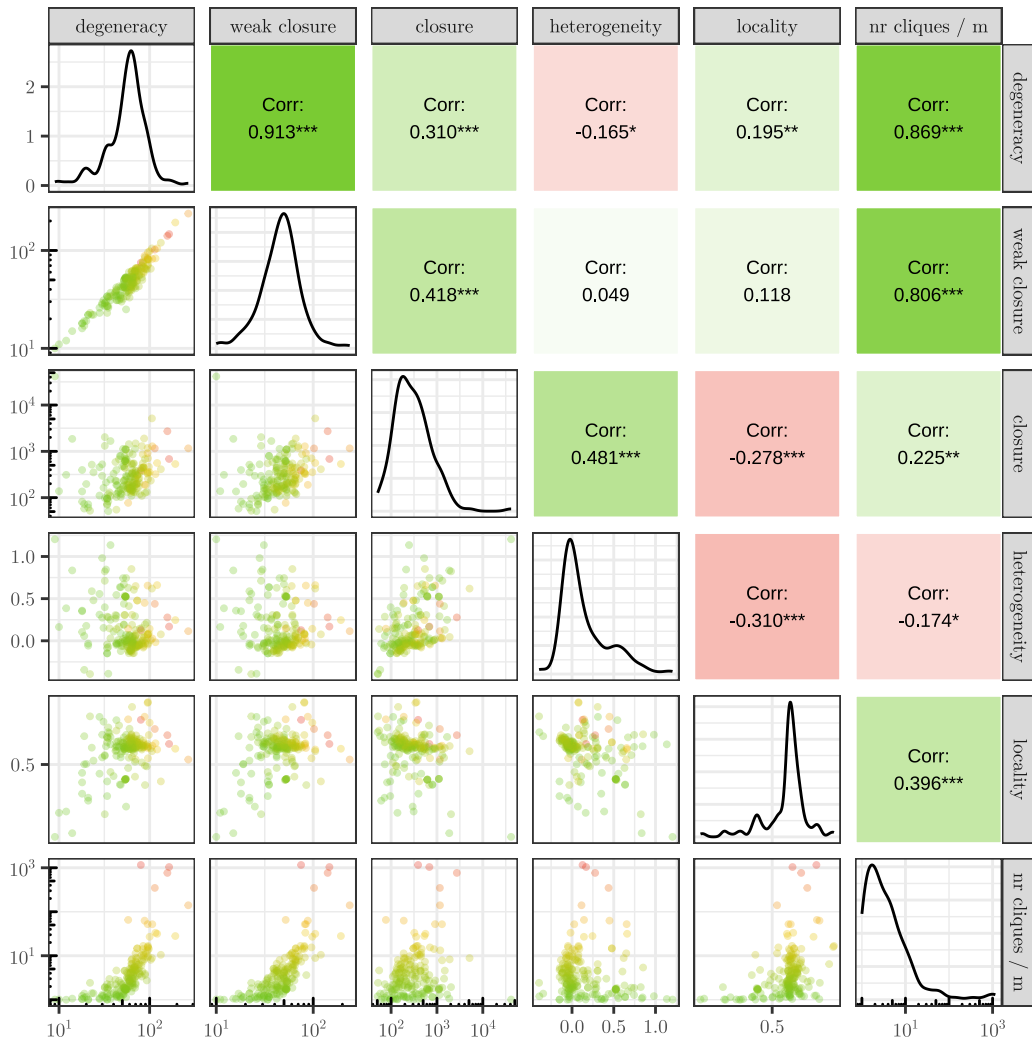


Figure 16 Pairwise comparison of different variables for the networks with at most m cliques. The upper triangle shows the Spearman correlation between the two corresponding variables. The colors go from green (positive correlation) over white (no correlation) to red (negative correlation). The stars indicate p-values (“***”: < 0.001 , “**”: < 0.01 , “*”: < 0.05 , “.”: < 0.1 , “ ”: otherwise). The diagonal shows the density of each individual variable. The lower triangle shows scatter plots of the networks with respect to two variables. The colors indicate the number of cliques (relative to m). Axes for degeneracy, weak closure, and closure are logarithmic.

$O(dn3^{d/3})$ [26] and $n^23^{(c-1)/3}$ [29], where d is the degeneracy and c the weak closure. For the closure on the other hand, there is only a slight correlation.

E.4 Relation Between the Parameters

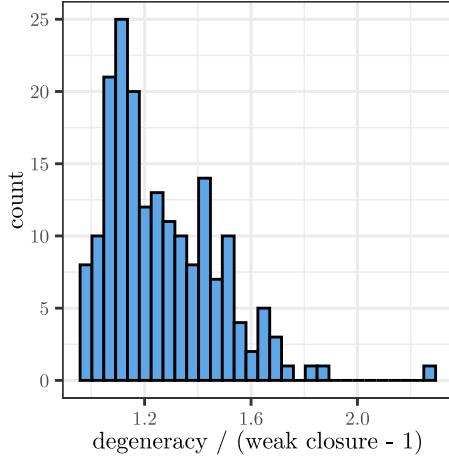
Besides studying the number of cliques with respect to the different parameters, it is also interesting to compare the parameters with each other. Closure and weak closure have both been introduced to formalize the same concept (triadic closure), thus one would suspect them to be similar. Moreover, recall that the weak closure and the degeneracy are both defined via elimination orders on the vertices and that $c - 1 \leq d$ for weakly c -closed graphs with



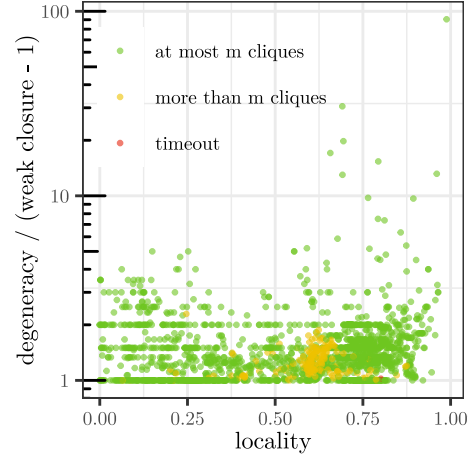
■ **Figure 17** Pairwise comparison as in Figure 16 but for the networks with more than m cliques. In addition to degeneracy, weak closure, and closure, the axis for the relative number of cliques is logarithmic.

degeneracy d . Thus, one can expect them to be similar on networks with few triangles. For graphs with many triangles (high locality), it is interesting to see whether the weak closure captures the concept of triadic closure well, i.e., whether $c - 1$ is substantially smaller than d .

Though the study of the relation between these parameters is independent of the number of cliques, we still consider the partition into networks with at most or more than m cliques for the following reason. Our interest in degeneracy and (weak) closure comes from trying to understand how many cliques a network has. As we have seen before, these parameters do not work well in this regard for networks with at most m cliques, i.e., they are more relevant for the networks with more than m cliques. If we, however, would consider all networks together, the networks with at most m cliques would dominate the overall picture as they make up 93% of all networks.



■ **Figure 18** Distribution of the relative difference between degeneracy and weak closure values for the networks with more than m cliques.



■ **Figure 19** Relative difference between degeneracy and weak closure depending on the locality. They show only a slight correlation (0.10 for networks with at most m cliques and 0.24 for networks with more than m cliques).

E.4.1 Networks With at Most m Cliques.

We can see in Figure 16 that degeneracy, closure, and weak closure are all positively correlated. We can also see that the degeneracy and the weak closure range in the same order of magnitude, while the closure is orders of magnitude larger.

Concerning correlation to heterogeneity and locality, we can observe a slight positive correlation of all three with the heterogeneity. This makes sense as all three parameters can only be high if there are vertices of high degree. Moreover, the correlation with locality is weaker or not present at all. For the (weak) closure, this is unexpected as they are meant to capture the existence of many triangles, which corresponds to a high locality. It is particularly surprising that there is a slight positive correlation of the weak closure with locality, i.e., a higher locality tends to lead to a larger weak closure, which is the opposite of what one would expect.

A possible explanation for this can be obtained by observing that closure focuses on non-edges while our definition of locality focuses on edges. Slightly simplifying, this difference can be stated as follows.

high locality: $\{u, v\} \in E \rightarrow u$ and v have many common neighbors

small closure: $\{u, v\} \notin E \rightarrow u$ and v do not have many common neighbors

E.4.2 Networks With More Than m Cliques.

For the networks where the degeneracy and weak closure were a good predictor for the number of cliques, we see an even stronger correlation between these two parameters. To quantify how much the degeneracy and the weak closure differ, see Figure 18. One can see that the weak closure is usually not much smaller than the upper bound given by the degeneracy. Thus, the weak closure is indeed very similar to the degeneracy. Hence it mostly captures the sparsity of a network rather than the tendency to have many triangles.

On these networks the correlation of the closure to degeneracy and weak closure is

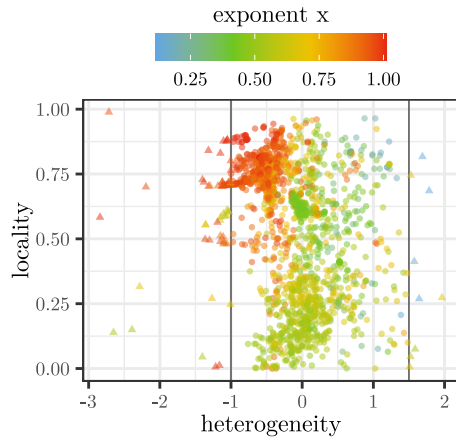
less pronounced than for the networks with at most m cliques. Concerning locality and heterogeneity, there is no correlation with degeneracy or weak closure. The closure correlates positively with heterogeneity and to a smaller extent negatively with locality. As for the other set of networks, this again indicates that the parameter closure is more susceptible to the degree distribution than to the existence of triangles.

E.4.3 Weak Closure and Locality

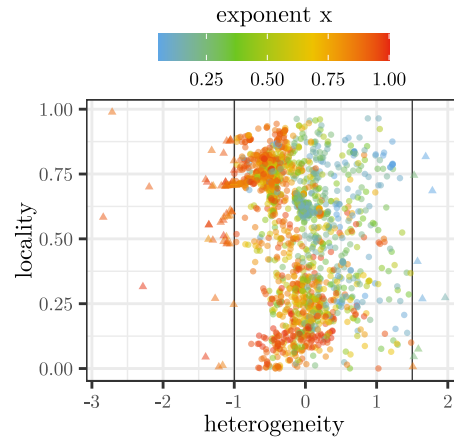
As mentioned earlier, the correlation between weak closure and degeneracy is not surprising as degeneracy is an upper bound to weak closure (minus 1). Here we want to study whether the difference between these two is correlated with the locality. If this difference comes mostly from the existence of many triangles, then one would expect a bigger difference for graphs with high locality. However, Figure 19 shows that this is not really the case. This consolidates the previous observation that (weak) closure does not capture the concept of locality well.

F Networks with Extreme Heterogeneity

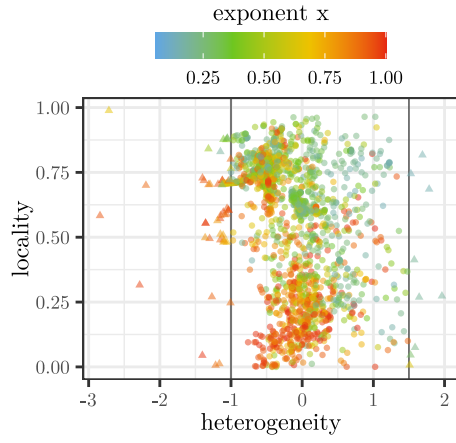
In this section, we provide the figures from Section 4 including real-world networks with extreme heterogeneity. Figure 20 and Figure 21 show the respective middle plots; the thresholds for extreme heterogeneity are marked with vertical lines, with triangle-shaped data points representing real-world networks with extreme heterogeneity, i.e., data points outside the thresholds. Across all considered algorithms, the behavior on networks with extreme heterogeneity roughly follows those of the other networks, showing similar trends of algorithm behavior dependence on locality and heterogeneity.



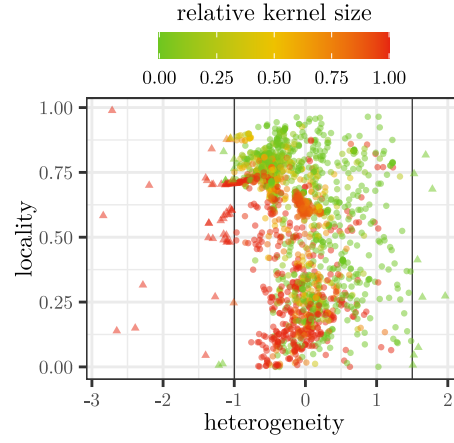
(a) Figure 4 (bidirectional BFS)



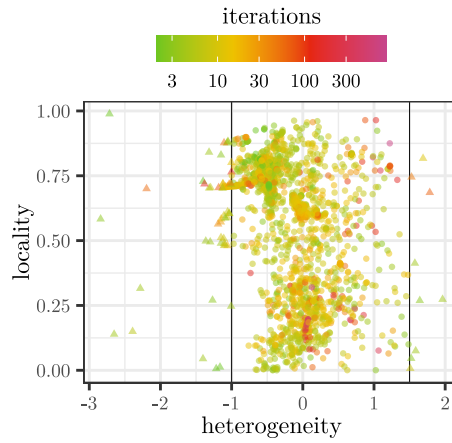
(b) Figure 5a (iFUB+hd)



(c) Figure 5b (iFUB+4-sweep)

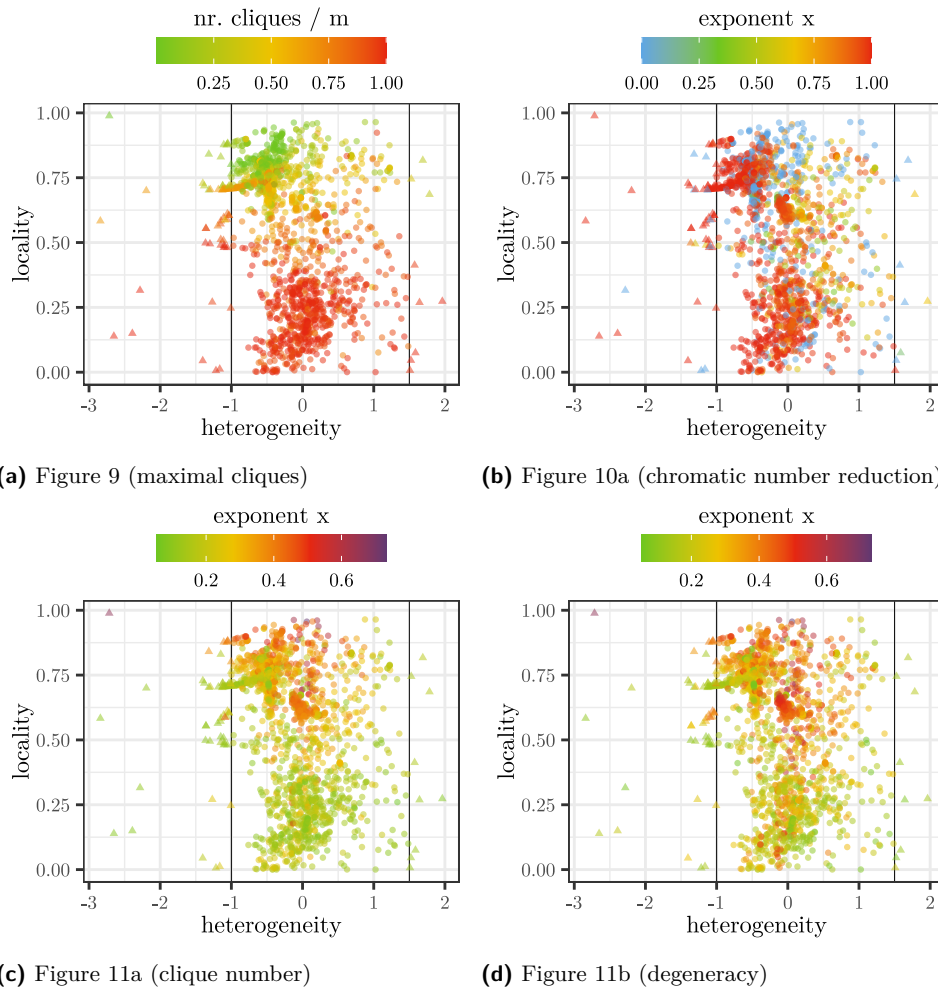


(d) Figure 7 (vertex cover domination)



(e) Figure 8 (Louvain)

■ **Figure 20** Full versions of the middle plots of several figures from Section 4 including real-world networks with extreme heterogeneity. The thresholds for extreme heterogeneity are marked with vertical lines, with triangle-shaped data points representing real-world networks with extreme heterogeneity.



■ **Figure 21** Additional full versions of the middle plots of several figures from Section 4 including real-world networks with extreme heterogeneity. The thresholds for extreme heterogeneity are marked with vertical lines, with triangle-shaped data points representing real-world networks with extreme heterogeneity.